JGR Biogeosciences

RESEARCH ARTICLE
10.1029/2023JG007853

Controls on the Respiration of Ancient Carbon Draining From Permafrost Soils Into Sunlit Arctic Surface Waters

E. C. Rieb[1], C. A. Polik[1,2], C. P. Ward[3], G. W. Kling[4], and R. M. Cory[1]

[1]Department of Earth and Environmental Sciences, University of Michigan, Ann Arbor, MI, USA, [2]Now at Department of Ecology, Evolution, and Behavior, University of Minnesota, St. Paul, MN, USA, [3]Department of Marine Chemistry and Geochemistry, Woods Hole Oceanographic Institution, Woods Hole, MA, USA, [4]Department of Ecology and Evolutionary Biology, University of Michigan, Ann Arbor, MI, USA

Key Points:

- Microbes respire ancient, ^{13}C-depleted dissolved organic carbon (DOC) from permafrost soils to carbon dioxide
- Effects of sunlight exposure on the amount of permafrost DOC respired depend on the extent of DOC oxidation by each wavelength of light
- Sunlight exposure of permafrost DOC can increase or decrease microbial respiration in arctic lakes and streams

Supporting Information:

Supporting Information may be found in the online version of this article.

Correspondence to:

R. M. Cory,
rmcory@umich.edu

Citation:

Rieb, E. C., Polik, C. A., Ward, C. P., Kling, G. W., & Cory, R. M. (2024). Controls on the respiration of ancient carbon draining from permafrost soils into sunlit arctic surface waters. *Journal of Geophysical Research: Biogeosciences*, *129*, e2023JG007853. https://doi.org/10.1029/2023JG007853

Received 24 OCT 2023
Accepted 10 APR 2024

Author Contributions:

Conceptualization: E. C. Rieb, C. A. Polik, C. P. Ward, G. W. Kling, R. M. Cory
Data curation: E. C. Rieb
Formal analysis: E. C. Rieb
Funding acquisition: E. C. Rieb, C. P. Ward, G. W. Kling, R. M. Cory
Investigation: E. C. Rieb, C. A. Polik, C. P. Ward
Methodology: E. C. Rieb, C. A. Polik, C. P. Ward, G. W. Kling, R. M. Cory
Resources: C. P. Ward, G. W. Kling, R. M. Cory
Software: E. C. Rieb, C. A. Polik
Supervision: C. P. Ward, G. W. Kling, R. M. Cory
Validation: E. C. Rieb, C. P. Ward
Visualization: E. C. Rieb, R. M. Cory

Abstract

The thawing of ancient organic carbon stored in arctic permafrost soils, and its oxidation to carbon dioxide (CO_2, a greenhouse gas), is predicted to amplify global warming. However, the extent to which organic carbon in thawing permafrost soils will be released as CO_2 is uncertain. A critical unknown is the extent to which dissolved organic carbon (DOC) from thawing permafrost soils is respired to CO_2 by microbes upon export of freshly thawed DOC to both dark bottom waters and sunlit surface waters. In this study, we quantified the radiocarbon age and ^{13}C composition of CO_2 produced by microbial respiration of DOC that was leached from permafrost soils and either kept in the dark or exposed to ultraviolet and visible wavelengths of light. We show that permafrost DOC most labile to microbial respiration was as old or older (ages 4,000–11,000 a BP) and more ^{13}C-depleted than the bulk DOC in both dark and light-exposed treatments, likely indicating respiration of old, ^{13}C-depleted lignin and lipid fractions of the permafrost DOC pool. Light exposure either increased, decreased, or had no effect on the magnitude of microbial respiration of old permafrost DOC relative to respiration in the dark, depending on both the extent of DOC oxidation during exposure to light and the wavelength of light. Together, these findings suggest that photochemical changes affecting the lability of permafrost DOC during sunlight exposure are an important control on the magnitude of microbial respiration of permafrost DOC in arctic surface waters.

Plain Language Summary

Organic carbon has been frozen in arctic permafrost soils for thousands of years. As these soils warm and thaw, the vast stores of ancient organic carbon they contain can amplify global warming if the carbon is converted to carbon dioxide (a greenhouse gas) in both dark soils and when drained into sunlit lakes and streams. However, quantifying the carbon dioxide produced from thawed permafrost organic carbon requires understanding the controls on this conversion. Here we show that native permafrost microbes can respire permafrost organic carbon to carbon dioxide both in the dark and after carbon exposure to different wavelengths of light. The carbon dioxide produced was as old as the organic carbon in the soil, suggesting that even ancient carbon can be respired by microbes. This study suggests that respiration by microbes will contribute to the rapid conversion of ancient permafrost organic carbon to carbon dioxide in sunlit arctic surface waters, further amplifying global warming.

1. Introduction

Permafrost soils are thawing in many regions of the Arctic (e.g., Jorgenson et al., 2006; Osterkamp, 2007; Smith et al., 2022; Zhao et al., 2020). Once thawed, the ancient organic carbon in permafrost soils can be respired to carbon dioxide (CO_2, a greenhouse gas; Schuur et al., 2015; Vaughn & Torn, 2019), contributing to the arctic amplification of climate change (McGuire et al., 2018). Permafrost thaw and thaw slump disturbances (thermokarsts; Kokelj & Jorgenson, 2013; Olefeldt et al., 2016) may also increase the lateral export of old, previously-frozen dissolved organic carbon (DOC) from permafrost soils to surface waters (Frey & McClelland, 2009; McFarlane et al., 2022; Plaza et al., 2019). DOC draining from permafrost soils to arctic streams is labile to microbial respiration (Drake et al., 2015; Mann et al., 2015; Spencer et al., 2015), particularly after the composition of this DOC has been altered by sunlight exposure (i.e., coupled photochemical and microbial degradation of DOC; Cory et al., 2013; Ward et al., 2017).

In arctic freshwaters, coupled photochemical and microbial degradation of DOC may account for over 90% of the total DOC processed in the water column (Cory et al., 2014). Sunlight has a strong influence on DOC composition and thus on its respiration to CO_2 in arctic waters due to high concentrations of sunlight-absorbing

Writing – original draft: E. C. Rieb, R. M. Cory
Writing – review & editing: E. C. Rieb, C. A. Polik, C. P. Ward, G. W. Kling, R. M. Cory

(chromophoric) DOC (CDOM) that absorb all or nearly all incoming ultraviolet (UV) and visible sunlight in the water column (Cory et al., 2014, 2015). Rates of sunlight degradation of DOC are not strongly influenced by water column depth, mixing, or turbidity in arctic surface waters (Cory et al., 2015; Cory & Kling, 2018; Li et al., 2019). Further, permafrost DOC is readily degraded by even the less energetic visible wavelengths of sunlight (Bowen et al., 2020b; Ward & Cory, 2016).

Most of the permafrost DOC degraded by UV and visible sunlight remains in the DOC pool as partially oxidized or chemically-altered compounds (Stubbins et al., 2017; Ward & Cory, 2016, 2020). Thus, even after sunlight degradation, permafrost DOC may be detected by its radiocarbon age in surface waters, as reported in headwater streams impacted by thawing permafrost (Mann et al., 2015; Neff et al., 2006; Spencer et al., 2015; Vonk et al., 2013) and in one major arctic river (Schwab et al., 2020). As permafrost DOC is increasingly exposed to sunlight during transport from streams to rivers, its lability to microbes should increase (Cory et al., 2013; Ward et al., 2017), promoting its respiration to CO_2. Consistent with this expected loss of permafrost DOC by coupled photochemical and microbial degradation, most studies have reported little to no old DOC in major arctic rivers receiving DOC from streams impacted by permafrost thaw (Aiken et al., 2014; Neff et al., 2006; Rogers et al., 2021; Wild et al., 2019).

In addition to loss of permafrost DOC by coupled photochemical and microbial degradation, preferential degradation of the oldest fractions of the permafrost DOC by these processes could mask the presence of ancient DOC in streams. Permafrost DOC is a mixture of thousands of compounds that span a range of ages (e.g., Rogers et al., 2021). There is evidence that older DOC is selectively respired relative to modern DOC in rivers and lakes (Mann et al., 2015; McCallister & del Giorgio, 2012). McCallister and del Giorgio (2012) hypothesized that selective respiration of relatively old DOC was due to its degradation by sunlight. For the mixture of DOC ages found in permafrost DOC, this hypothesis is supported by evidence that sunlight degradation of permafrost DOC produced the same low molecular weight, aliphatic DOC compounds most labile to microbial respiration in the dark (Nalven et al., 2020; Ward et al., 2017). However, it is not known whether sunlight exposure makes relatively older or younger compounds within the old permafrost DOC pool more labile to microbes.

The ^{13}C composition of the permafrost DOC respired by microbes, in addition to the age, may characterize the chemical composition of permafrost DOC most labile to microbes. Prior work showed that the fraction of permafrost DOC respired by microbes in the dark has a ^{13}C composition that is similar to the bulk DOC (Mann et al., 2015; Spencer et al., 2015). A null interpretation of these results is that all ^{13}C compositions of permafrost DOC are similarly labile to microbial respiration. Another interpretation is that the relatively large amount of DOC respired masked any preferential respiration of labile fractions of DOC differing in their ^{13}C composition compared to the bulk permafrost DOC. For example, prior studies used warm incubations (20°C) supporting high respiration rates and consumption of up to 50% of the DOC. As the amount of DOC consumed increases, the isotopic signature of the CO_2 produced should increasingly match the average isotopic signature of the bulk DOC. Therefore, the similarity between the ^{13}C composition of the bulk and respired permafrost DOC in prior work does not necessarily imply that all fractions of the bulk permafrost DOC are similarly labile to microbial respiration. In contrast, in arctic surface waters impacted by permafrost thaw, such as small headwater streams, conditions including ice-free average water temperatures of 3–12°C (Adams et al., 2010; Cory et al., 2014; Docherty et al., 2019), short residence times, and rapid replenishment with fresh, terrestrial DOC (Cory et al., 2015; Neilson et al., 2018) may favor respiration of a smaller percentage of the DOC pool. Under these conditions, it is not known whether microbes selectively respire compound classes that are depleted or enriched in ^{13}C compared to the bulk DOC.

The respiratory quotient of DOC respired may also provide information on fractions of permafrost DOC most labile to microbes. This quotient of CO_2 produced to O_2 consumed during respiration is thought to depend on the oxidation state of the substrate respired (Masiello et al., 2008). Substrates with a lower average oxidation state of carbon are hypothesized to yield relatively less CO_2 per mol O_2 consumed compared to substrates having a higher average oxidation state of the carbon (Masiello et al., 2008; Pries et al., 2020). This hypothesis is based on respiratory quotients for glucose, oxalic acid, and other small organic compounds (Dilly, 2001; Theenhaus et al., 1997). While the respiratory quotients for larger or more heterogeneous DOC compounds like lipids or lignin-like DOC have not been tested, this hypothesis predicts that more reduced lipid and lignin-like compounds are respired with a lower respiratory quotient than more oxidized carbohydrates and organic acids (Dilly, 2001; Romero-Kutzner et al., 2015).

Finally, another major uncertainty preventing a quantitative assessment of the effects of sunlight exposure on respiration of permafrost DOC is the wavelength dependence of this process. The one study that has isolated the effects of individual wavelengths of light on DOC degradation reports substantial variability in both the direction and magnitude of the effects of ultraviolet (UV) and visible wavelengths of light on microbial respiration (Reader & Miller, 2014). Because more visible than UV photons of sunlight are absorbed by DOC, incorrect assumptions about the relative importance of UV and visible light for producing DOC labile to microbes can lead to a systematic under- or overestimation of CO_2 from microbial respiration in arctic surface waters.

To address these knowledge gaps, permafrost DOC spanning a range of ages and compositions was collected from younger and older glacial surfaces and from under two common vegetation types in the Alaskan Arctic. Permafrost DOC was exposed to UV and visible wavelengths of LED-generated light, alongside dark controls. Following light exposure, biological incubations at water temperatures of arctic surface waters were conducted to make the first direct quantifications of the radiocarbon age of CO_2 produced by microbial respiration of ancient permafrost DOC, both in the dark and after light exposure. The ^{13}C composition of CO_2 from respiration and respiratory quotients were also quantified to characterize the composition of permafrost DOC most labile to microbes.

2. Materials and Methods

2.1. Soil Collection

Permafrost soil cores were collected on the North Slope of Alaska during the ice-free summer months of June-August 2018 near the Toolik Field Station (Table S1 in Supporting Information S1). In the foothills of this region, mountain glaciations have produced land surfaces of different ages from relatively younger (~14,000 years BP since last glaciation) to relatively older (>250,000 years BP since last glaciation; Hamilton, 2003). Soil cores were collected from within the permafrost layer (at 85 cm below the surface and ~10–30 cm below the maximum summer thaw depth; see Romanowicz & Kling, 2022) of Imnavait Creek wet sedge (wet sedge) and Toolik Lake tussock tundra (tussock tundra) soils, which represent the dominant landscape ages and vegetation types of the low Arctic (Figure S1 and Table S1 in Supporting Information S1; Ping et al., 1998; Trusiak et al., 2018a; Walker et al., 2005; Walker & Maier, 2008). DOC leached from these soils has a range of chemical compositions and ages (Bowen et al., 2020b; Trusiak et al., 2018a; Ward et al., 2017). In June 2022, soil was sampled from a thermokarst failure on the shore of Lake LTER 395 on the North Slope of Alaska (referred to as "thermokarst"), where an abrupt collapse of thawing soil exposed deeper permafrost soil (Figure S1 and Table S1 in Supporting Information S1). Soil was sampled from the permafrost layer on a freshly-cleaned soil profile in the headwall of the thermokarst failure (>80 cm below the surface and ~10–30 cm below the maximum summer thaw depth) using MilliQ-rinsed pickaxes.

The permafrost and thermokarst soil samples were collected as previously described in detail (Bowen et al., 2020b), including precautions to minimize radiocarbon (^{14}C) contamination by rinsing gloves and tools with deionized water prior to soil collection and storing soil samples in ^{14}C-free facilities and freezers. These protocols were shown to result in no detectable ^{14}C contamination of soils (Bowen et al., 2020b). All soils were stored in freezers at the Toolik Field Station until overnight shipment to Woods Hole Oceanographic Institution (WHOI), where soils were stored in ^{14}C-free freezers until further use.

2.2. Soil Leachate Preparation and Characterization

DOC was leached from the permafrost and thermokarst soils as previously described (Bowen et al., 2020b). Briefly, frozen soil and UVC-oxidized MilliQ water (Table S2 in Supporting Information S1) were mixed in 5-gallon, MilliQ-rinsed HDPE buckets and allowed to leach in the dark for 1–4 days at 4°C. Both the soil-to-water ratio of soil leachates and the leaching time were adjusted to achieve a final concentration of ~500–1,500 μM DOC in the leachates, as estimated from the absorbance of chromophoric dissolved organic matter at 305 nm (a_{305}).

All leachates were passed through MilliQ-rinsed 60 μm mesh screens to remove the largest particulates and then through MilliQ-rinsed 5 μm high-capacity Whatman cartridge filters. Subsamples of each leachate for light exposure experiments were then filtered through 0.2 μm high-capacity cartridge filters to minimize microbial activity (Step A in Figure S2 in Supporting Information S1; Ward et al., 2017). Additional subsamples of each

Table 1
$\Delta^{14}C$ and $\delta^{13}C$ of Permafrost DOC and the CO_2 From Respiration of Permafrost DOC During Biological Incubations

	Treatment	Imnavait wet sedge tundra	Toolik tussock tundra A	Toolik tussock tundra B	LTER 395 thermokarst
Δ^{14}C-DOC (‰)	Dark	−594 ± 2	−502 ± 2	−441 ± 2	−433 ± 1
	UV	−589 ± 2	−502 ± 2	−432 ± 1	−440 ± 1
	Visible	−582 ± 2	−502 ± 2	−439 ± 2	−437 ± 1
Δ^{14}C-CO_2 respired (‰)	Dark	−689 ± 52		−668 ± 22	−448 ± 6
	UV	−572 ± 2	−740 ± 40	−597 ± 2	−415 ± 1
	Visible		−627 ± 16	−624 ± 4	−405 ± 0
^{14}C age of DOC (a BP)	Dark	7,170 ± 35	5,540 ± 30	4,610 ± 25	4,500 ± 20
	UV	7,080 ± 35	5,540 ± 30	4,470 ± 20	4,600 ± 20
	Visible	6,940 ± 35	5,540 ± 30	4,580 ± 20	4,560 ± 20
^{14}C age of CO_2 respired (a BP)	Dark	9,439 ± 1,360		8,815 ± 541	4,711 ± 81
	UV	6,755 ± 40	10,835 ± 1,240	7,229 ± 35	4,247 ± 10
	Visible		7,853 ± 339	7,793 ± 94	4,100 ± 5
δ^{13}C-DOC (‰)	Dark	−28.8	−25.3	−25.9	−26.3
	UV	−28.1	−25.6	−25.5	−25.9
	Visible	−28.2	−25.3	−25.7	−26.0
δ^{13}C-CO_2 respired (‰)	Dark	−40.2 ± 2.7		−31.9 ± 1.3	−32.2 ± 0.7
	UV	−37.3 ± 0.5	−44.9 ± 3.0	−29.9 ± 1.0	−28.5 ± 0.3
	Visible			−32.8 ± 0.6	−28.1 ± 0.2

Note. The Δ^{14}C and δ^{13}C of permafrost DOC are reported following dark treatment, UV light treatment (305 nm), or visible light treatment (405 nm), and subsequent inoculation. The Δ^{14}C and δ^{13}C of the CO_2 from respiration of permafrost DOC are reported following biological incubations. Values for DOC are reported with the instrumental error, and values for CO_2, when available, are reported as the average ±1 SE of experimental replicates ($n = 2$).

leachate were prepared as inoculum for biological incubations by passing the 5-μm-filtered water through 1.2 μm glass-fiber filters (hereafter referred to as the inoculum; Step B in Figure S2 in Supporting Information S1). All filters used to prepare leachates were rinsed with 5 L of MilliQ water before use. Leach tests for DOC contamination from the filters found that less than 5 μM DOC leached into MilliQ rinses from the Whatman and Sterivex filters. Thus, any ^{14}C contamination from filtering permafrost leachates was within the instrumental precision of the radiocarbon analyses (≤6‰; see Bowen et al., 2020b). Prior work following the same protocols as in this study for leachate preparation concluded that potential ^{14}C contamination during the soil leaching process before filtration was also within the instrumental precision of the radiocarbon analyses (Bowen et al., 2020b). Soil leachates for light exposure experiments and biological incubations were stored at 4°C until further use (less than 48 hr for light exposure experiments, and less than 1 week for biological incubations). Supporting soil leachate chemistry analyses (pH, specific conductivity, iron, DOC, and chromophoric and fluorescent dissolved organic matter) were performed as previously described (Bowen et al., 2020b; Cory et al., 2013, 2014; Kling et al., 2000).

Due to sample loss during experiments and ^{14}C analyses, duplicate leachates were prepared from the thermokarst and tussock tundra soils. From the thermokarst soil, the first leachate prepared was used for both UV and visible light treatments and the second leachate was used for the dark control. From the tussock tundra soil, there was sample loss from the first leachate (labeled A) for some of the dark and visible light treatment samples (Table 1). Thus, the second leachate prepared from the tussock tundra soil (labeled B) replaced the samples lost from leachate A and provided experimental duplicates for the samples analyzed from leachate A (Table 1). See Section S1.1 in Supporting Information S1 for details.

2.3. LED Light Exposure Experiments

Each 0.2-μm-filtered soil leachate was allowed to warm from the 4°C storage temperature to room temperature for 12–24 hr prior to the start of dark or light treatments. Each soil leachate was then placed in six precombusted, 500 mL quartz flasks with ground glass stoppers without headspace. For each soil leachate, duplicate quartz flasks

were exposed to 305 and 405 nm LED light treatments using custom-built 10 × 1 LED chip arrays maintained at 30°C using heat sinks and cooling fans (Bowen et al., 2020b; Ward et al., 2021). These wavelengths representing UV (305 nm) and visible (405 nm) sunlight were chosen because studies suggest that production of DOC photoproducts labile to microbial respiration is highest near 305 nm (Miller et al., 2002) and differs by wavelength (Reader & Miller, 2014; Wetzel et al., 1995). Duplicate dark controls were run alongside light treatments at room temperature (23°C) in the dark (Step C in Figure S2 in Supporting Information S1).

Changes in water chemistry and photochemical O_2 consumption during light exposure were measured as in prior work (Table S3 in Supporting Information S1, Ward & Cory, 2016). The amount of DOC oxidized to CO_2 during LED light exposures was estimated from photochemical O_2 consumption, assuming 1 mol DOC completely oxidized to CO_2 per mol O_2 consumed (Cory et al., 2014; Ward & Cory, 2020). This is a conservative estimate of the amount of DOC oxidized because the ratio of CO_2 produced per O_2 consumed is often >1 in high-DOC and high-iron waters similar to permafrost leachates (Bowen et al., 2020b; Ward & Cory, 2020). The durations of light exposures were chosen to achieve complete oxidation of ∼5%-10% of the initial DOC from all leachates and ranged from 20 to 120 hr depending on the soil site and wavelength (Table S3 in Supporting Information S1). Oxidation of 5%–10% of the DOC was chosen because prior work showed substantial microbial response (in both respiration and bacterial production) upon oxidation of <5% of the DOC (Nalven et al., 2020; Ward et al., 2017). In addition, short residence times in headwater streams impacted by permafrost thaw likely mean that only a small percent of the DOC is oxidized before export downstream (e.g., Cory & Kaplan, 2012). For each soil site, the same amount of DOC was oxidized by both UV and visible light (Table S3 in Supporting Information S1).

The duplicates of soil leachates from each dark or light treatment were composited in precombusted glass bottles (Step D in Figure S2 in Supporting Information S1) and stored overnight in the dark at 4°C before further use in biological incubations. This storage period allowed for decay of reactive oxygen species produced upon exposure of DOC to UV and visible light (Andrews et al., 2000; Cory et al., 2010; Page et al., 2014; White et al., 2003).

2.4. Biological Incubations

Each soil leachate treatment (dark, UV, visible) was mixed with the respective inoculum from each site to achieve 20% inoculum by volume (Cory et al., 2013; Step D in Figure S2 in Supporting Information S1). From each inoculated dark and light-exposed leachate, replicates for ^{14}C and ^{13}C analysis of the CO_2 produced by microbial respiration were filled in precombusted 125 mL borosilicate bottles with greased glass stoppers and no headspace (Step E in Figure S2 in Supporting Information S1). For each dark or light-exposed leachate, there were duplicate viable and killed treatments to quantify the C isotopic signatures of the CO_2 produced during respiration. The viable treatment was unamended, and the killed treatment was amended with saturated mercuric chloride (all preservations had 1% $HgCl_2$ by sample volume).

The amount of DOC respired from each dark and light-exposed leachate was quantified as O_2 consumption and CO_2 production by microbial respiration (Table S4 in Supporting Information S1). O_2 consumed and CO_2 produced by respiration were quantified as the difference in dissolved O_2 and dissolved inorganic carbon (DIC), respectively, between viable and killed treatments from a split of each inoculated dark and light-exposed leachate placed in precombusted, gas-tight 12 mL soda glass exetainers with no headspace (Step E in Figure S2 in Supporting Information S1). For each dark and light-exposed leachate, there were triplicate viable and killed treatments for analysis of O_2 and DIC. The viable treatment was unamended, and the killed treatment was amended with saturated mercuric chloride.

All viable and killed inoculated soil leachates were incubated in the dark at 10°C for between 17 and 30 days (Step E in Figure S2 and Table S4 in Supporting Information S1). This incubation temperature is representative of a typical, annual average temperature for non-frozen lakes and streams near soil sampling sites (Cory et al., 2014). The incubation duration was chosen for each set of dark and light-exposed soil leachates from a soil site so that respiration produced at least a 10% increase in the total DIC of the water compared to the start of the incubation (Table S4 in Supporting Information S1). A 10% increase in the total DIC was chosen so that the ^{14}C and ^{13}C isotopic compositions of the CO_2 produced by microbial respiration were detectable against the isotopic compositions of the background DIC in the soil leachates. At the end of the incubations, all viable leachate treatments in 125 mL borosilicate bottles and 12 mL exetainers were preserved by addition of saturated mercuric chloride. These preserved samples were stored at 4°C in the dark until ^{14}C and ^{13}C analysis (up to 2 months) or until analysis of O_2 consumption and CO_2 production by respiration (less than 2 weeks) as previously described

(Bowen et al., 2020b; Cory et al., 2014). Respiratory quotients were calculated as the ratio of CO_2 production to O_2 consumption by microbial respiration.

2.5. $\Delta^{14}C$ and $\delta^{13}C$ of DOC

A 75 mL sample of each soil leachate after dark or light treatment and inoculation (Step D in Figure S2 in Supporting Information S1) was 0.22-μm Sterivex filtered and frozen for ^{14}C and ^{13}C analysis of the DOC present at the start of the biological incubations (Table 1 and Table S5 in Supporting Information S1). The $\Delta^{14}C$ and $\delta^{13}C$ of the DOC were quantified at the National Ocean Sciences Accelerator Mass Spectrometry (NOSAMS) Facility at WHOI, using previously described methods (Xu et al., 2021). Briefly, soil leachates were acidified to pH < 2 with UVC-oxidized trace-metal grade phosphoric acid (85%) and stripped of dissolved inorganic carbon (DIC) with high-purity helium gas in the dark. The DOC was then oxidized with UVC light to DIC, and the resultant CO_2 was extracted cryogenically. A subsample of the CO_2 was analyzed for ^{13}C using a VG Prism-II or Optima stable isotope ratio mass spectrometer, and the $\delta^{13}C$ (‰) was calculated as follows:

$$\delta^{13}C = \left({}^{13}R_{sample} \Big/ {}^{13}R_{standard} - 1\right)$$

where ^{13}R is the isotope ratio of a sample or standard (VPDB), as defined by:

$${}^{13}R = \left({}^{13}C \Big/ {}^{12}C\right)$$

The remaining CO_2 was reduced to graphite with H_2 and an iron catalyst, and then analyzed for ^{14}C isotopic composition using an accelerator mass spectrometer at the NOSAMS facility (Longworth et al., 2015). The $\Delta^{14}C$ (‰) and radiocarbon age of DOC were calculated from the fraction modern using the oxalic acid I standard (NIST-SRM 4990).

2.6. $\Delta^{14}C$ and $\delta^{13}C$ of CO_2 From Microbial Respiration

To characterize the isotopic composition of the DOC respired by microbes, the $\Delta^{14}C$ and $\delta^{13}C$ of dissolved inorganic carbon (DIC) were quantified in duplicate at NOSAMS from the viable and killed treatments of each dark and light-exposed leachate at the end of the incubation (after Step E in Figure S2 in Supporting Information S1), following procedures previously described for quantification of the $\Delta^{14}C$ and $\delta^{13}C$ of CO_2 produced from photomineralization of permafrost DOC (Bowen et al., 2020b). Water samples were acidified as described in Section 2.5 and stripped of DIC using high-purity nitrogen gas. The ^{14}C and ^{13}C of the resultant, trapped and purified CO_2 were analyzed at the NOSAMS facility and converted to $\Delta^{14}C$ and $\delta^{13}C$ values as described in Section 2.5.

The $\Delta^{14}C$ and $\delta^{13}C$ of CO_2 produced by microbial respiration of permafrost DOC ($\Delta^{14}C_{resp}$ and $\delta^{13}C_{resp}$) were calculated as follows:

$$\Delta^{14}C_{resp} = \frac{\left(\Delta^{14}C_{Viable} \times [DIC]_{Viable}\right) - \left(\Delta^{14}C_{Kill} \times [DIC]_{Kill}\right)}{[DIC]_{Viable} - [DIC]_{Kill}}$$

$$\delta^{13}C_{resp} = \frac{\left(\delta^{13}C_{Viable} \times [DIC]_{Viable}\right) - \left(\delta^{13}C_{Kill} \times [DIC]_{Kill}\right)}{[DIC]_{Viable} - [DIC]_{Kill}}$$

The $\Delta^{14}C$ and $\delta^{13}C$ of CO_2 produced by microbial respiration of permafrost DOC are reported as the average ± 1 standard error (SE) of duplicate viable treatments relative to duplicate killed controls (Table 1 and Table S5 in Supporting Information S1). See Section S1.2 in Supporting Information S1 for details about statistical analyses.

3. Results

3.1. DOC and Leachate Characterization

All soil leachates were relatively dilute (specific conductivity 8 to 24 μS cm^{-1}; Table S2 in Supporting Information S1), mildly acidic (pH 5.5 to 6.8, Table S2 in Supporting Information S1), and relatively high in both DOC

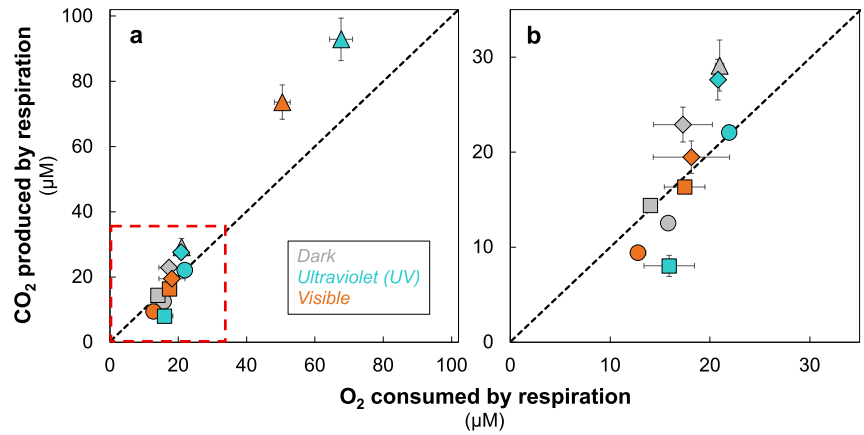

Figure 1. CO_2 produced versus O_2 consumed by microbial respiration of DOC kept in the dark (gray), exposed to ultraviolet light (UV; 305 nm, teal), and exposed to visible light (405 nm, orange) for: Imnavait wet sedge tundra (circle symbols), Toolik tussock tundra A (square symbols), Toolik tussock tundra B (diamond symbols), and LTER 395 thermokarst (triangle symbols). Panel (a) shows all of the data, and the region outlined in red is enlarged in panel (b). Data are plotted with the 1:1 line (dashed). Values for CO_2 production and O_2 consumption are shown as the average ±1 SE of experimental replicates ($n = 3$). When no error bars are visible, they are smaller than the data point symbols.

concentration (609–1,726 μM C; Table S2 in Supporting Information S1) and total dissolved iron concentration (3.1–22.2 μM iron) compared to most arctic surface waters that are not directly impacted by permafrost thaw (Aiken et al., 2014; Cory et al., 2013, 2014). The composition of the DOC in all leachates was characteristic of DOC draining from permafrost soils based on the relatively low $SUVA_{254}$ and high fluorescence index (Abbott et al., 2014; Cory et al., 2013; Mann et al., 2014; Spencer et al., 2015; Stubbins et al., 2017). Compared to pore waters from the upper, thawed soil layer at the same sites in the Alaskan Arctic, the permafrost soil leachates had lower conductivity but similar pH and DOC concentrations (Page et al., 2013, 2014; Trusiak et al., 2018a, 2018b). Thus, the composition of the permafrost leachates in this study was similar to the composition of both streams and soil pore waters in permafrost tundra.

3.2. Respiration of DOC

Respiration produced from 8 ± 1 to 93 ± 7 μM CO_2 (mean ± 1 SE) over the 17 to 30-day incubations at 10°C for all dark and light-exposed soil leachates (Figure 1, Table S4 in Supporting Information S1), which was from 0.7 ± 0.1 to 5.4 ± 0.4% of the initial DOC. The rate of CO_2 production was significantly, positively correlated with the DOC concentration at the start of the incubation (Figure S4 in Supporting Information S1, $p < 0.01$).

Light exposure increased, decreased, or did not change the amount of DOC respired to CO_2 compared to respiration of DOC kept in the dark, with the effect of light differing by wavelength and by soil site. For the wet sedge, tussock tundra B, and thermokarst soil leachates, microbial respiration was 76%, 16%, and 219% higher, respectively, in the UV light treatment than in the dark treatment (Figure 1, Figure S3 in Supporting Information S1). Respiration from the tussock tundra A leachate was 44% lower in the UV treatment than in the dark treatment. For the thermokarst and tussock tundra A leachates, respiration was 153% and 14% higher, respectively, in the visible light treatments than in the dark treatment (Figure 1, Figure S3 in Supporting Information S1). Respiration from the wet sedge leachate was 25% lower in the visible light treatment than in the dark treatment. For the tussock tundra B leachate, there was no significant difference in respiration between the UV and visible treatments and the dark treatment (Figure 1, Figure S3 in Supporting Information S1).

The respiratory quotient (the ratio of CO_2 production to O_2 consumption by microbial respiration) for respiration of DOC from the dark and light-exposed soil leachates ranged from 0.61 ± 0.16 to 1.47 ± 0.15 (Figure S3 and Table S4 in Supporting Information S1). Microbes respired UV-exposed wet sedge DOC with a significantly higher respiratory quotient compared to the dark DOC from this soil site. In contrast, microbes respired UV-exposed tussock tundra A DOC with a lower respiratory quotient compared to the dark DOC. For the tussock tundra B and thermokarst leachates, the respiratory quotient was not significantly different between dark and UV-

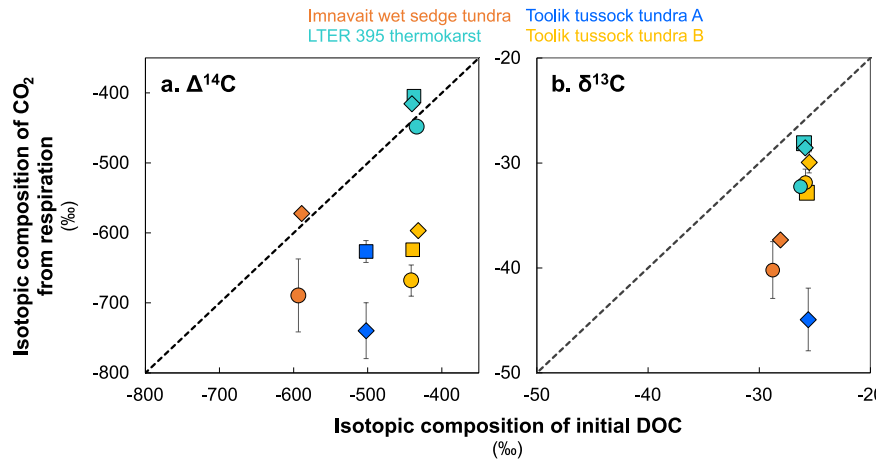

Figure 2. (a) $\Delta^{14}C$ composition and (b) $\delta^{13}C$ composition of CO_2 produced from microbial respiration of DOC kept in the dark (circle symbols), exposed to ultraviolet light (UV; 305 nm, diamond symbols), and exposed to visible light (405 nm, square symbols) versus the composition of the initial DOC of dark or light-exposed permafrost DOC for: Imnavait wet sedge tundra (orange symbols), Toolik tussock tundra A (dark blue symbols), Toolik tussock tundra B (yellow symbols), and LTER 395 thermokarst (teal symbols). Data are plotted with the 1:1 line (dashed). Values for $\Delta^{14}C$-CO_2 and $\delta^{13}C$-CO_2 are shown as the average ±1 SE of experimental replicates ($n = 2$).

light exposed DOC. Unlike UV light, visible light exposure resulted in no significant difference in respiratory quotient compared to the dark DOC for any soil sites.

3.3. $\Delta^{14}C$ of Initial and Respired DOC

The age of the DOC in the soil leachates after dark or light treatment and inoculation (Step D in Figure S2 in Supporting Information S1) ranged from ~4,500 a BP for thermokarst and tussock tundra A and B DOC to ~7,000 a BP for wet sedge DOC (Table 1). DOC in leachates of soils collected from the younger-age landscape (tussock tundra A, tussock tundra B, and thermokarst; Table S1 in Supporting Information S1) was younger than the DOC in the wet sedge leachate, which was collected from the older-age landscape. The CO_2 from respiration in all dark and light-exposed leachates had a wider range in age than did the DOC, from 4,100 to 10,835 a BP (Table 1). There was no significant correlation between the $\Delta^{14}C$ of the DOC and the $\Delta^{14}C$ of the CO_2 from respiration (Figure 2a, Table 1).

For all of the soil leachates paired with a dark control, CO_2 from respiration of light-exposed DOC was younger than the CO_2 from respiration of DOC kept in the dark. The degree to which CO_2 from respiration of light-exposed DOC was enriched in ^{14}C relative to respiration of DOC kept in the dark ranged from 33 ± 6‰ for UV-treated thermokarst leachate to 117 ± 54‰ for UV-treated wet sedge leachate (Figure 2a).

For the majority of the soil leachates that were exposed to both UV and visible light, there was no wavelength-dependent effect of light on the ^{14}C isotopic composition of the CO_2 from respiration. The exception to this result was the tussock tundra A leachate, for which the CO_2 from the visible light treatment was significantly enriched in ^{14}C compared to the CO_2 from the UV light treatment (Figure 2a). For the thermokarst and tussock tundra B leachates, there was little to no significant difference in the ^{14}C isotopic composition of the CO_2 from respiration between the UV and visible light treatments (Figure 2a).

3.4. $\delta^{13}C$ of Initial and Respired DOC

The ^{13}C isotopic composition of the DOC in the leachates after dark or light treatment and inoculation (Step D in Figure S2 in Supporting Information S1) ranged from −28.8‰ to −25.5‰ (Table 1). Wet sedge DOC was the most ^{13}C-depleted (−28.4 ± 0.2‰), while thermokarst and tussock tundra DOC were relatively more ^{13}C-enriched (−26.0 ± 0.1 and −25.7 ± 0.1‰, respectively; Table 1). The CO_2 produced by microbial respiration of permafrost DOC had a substantially wider range of ^{13}C isotopic compositions than did the DOC, from −44.9‰ to −28.1‰, and was always depleted relative to the DOC by 2–19‰ (Table 1). There was no significant correlation between the $\delta^{13}C$ of the DOC and the $\delta^{13}C$ of CO_2 from respiration (Figure 2b, Table 1). The $\delta^{13}C$ of CO_2

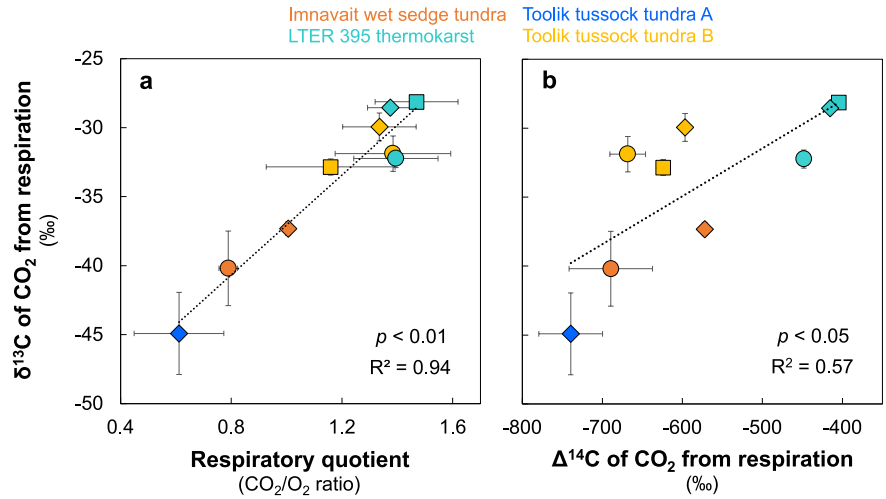

Figure 3. δ^{13}C-CO_2 produced from microbial respiration of DOC kept in the dark (circle symbols), exposed to ultraviolet light (UV; 305 nm, diamond symbols), and exposed to visible light (405 nm, square symbols) increased with (a) increasing respiratory quotient and (b) decreasing age of the CO_2 from: Imnavait wet sedge tundra (orange symbols), Toolik tussock tundra A (dark blue symbols), Toolik tussock tundra B (yellow symbols), and LTER 395 thermokarst (teal symbols). In panel (a), data were fit using a least-squares regression where $R^2 = 0.94$ and $p < 0.01$. All values on the x-axis are shown as the average ±1 SE ($n = 3$). All values on the y-axis are shown as the average ±1 SE ($n = 2$). In panel (b), data were fit using a least-squares regression where $R^2 = 0.57$ and $p < 0.05$. All values on the x- and y-axes are shown as the average ±1 SE ($n = 2$).

from respiration in dark and light-exposed soil leachates was significantly, positively correlated with both the respiratory quotient (Figure 3a) and the Δ^{14}C of the CO_2 from respiration (Figure 3b).

For the wet sedge and tussock tundra B soil leachates, light exposure had no significant effect on the ^{13}C isotopic composition of the CO_2 from respiration compared to respiration of DOC kept in the dark (Figure 2b). For the thermokarst leachate, the CO_2 from respiration in UV and visible light treatments was significantly enriched in ^{13}C compared to the CO_2 from respiration in the dark treatment. For all of the soil leachates that were exposed to both UV and visible light, there was little to no wavelength-dependent effect of light on the ^{13}C isotopic composition of the CO_2 from respiration (Figure 2b).

4. Discussion

These first quantifications of the age of CO_2 produced by microbial respiration of permafrost DOC (Figure 2a) show that microbes can respire ancient permafrost DOC to CO_2 upon export of this carbon to sunlit surface waters, as expected from prior work (Cory et al., 2013). This result is consistent with prior studies that quantified the age of permafrost DOC respired in the dark based on changes in the bulk DOC age (Mann et al., 2015; Spencer et al., 2015). Together, these results and prior work demonstrate that permafrost DOC is labile to microbial respiration in arctic surface waters, whether it is freshly thawed from dark soils (this study; Mann et al., 2015; Melchert et al., 2022; Spencer et al., 2015) or has been exposed to UV and visible sunlight (this study).

While the permafrost DOC respired by microbes was always old (>4,000 a BP), microbial respiration consistently produced younger CO_2 from light-exposed DOC than from dark controls. There are several potential explanations for this result. First, sunlight might completely oxidize relatively older DOC, leaving behind relatively younger DOC for microbes to respire. Studies exposing DOC from marine and lower-latitude freshwaters to high doses of UV light have found that younger DOC is preferentially oxidized to CO_2 by sunlight (Beaupré & Druffel, 2012; Beaupré et al., 2007; Ishikawa et al., 2019). However, for permafrost DOC exposed to environmentally-relevant, lower doses of UV and visible light, the age of the DOC completely oxidized to CO_2 by light has been shown to be similar to the age of the bulk permafrost DOC (≤70‰, or ≤930 years, different from the bulk DOC; Bowen et al., 2020b). This result, combined with the small amount of DOC completely oxidized to CO_2 by sunlight prior

to the incubation (Table S3 in Supporting Information S1), suggests that complete oxidation of DOC during light exposure should not cause substantial changes in the average age of the bulk DOC available for microbes to respire.

Second, light might cause microbes to respire younger DOC by altering the composition of the DOC remaining after light exposure (Bowen et al., 2020a; Cory et al., 2010; Ward & Cory, 2016; Wetzel et al., 1995), either by making younger DOC more labile or older DOC less labile compared to the same age fractions kept in the dark. These changes in the lability of different DOC age fractions would represent an increase or decrease in the amount of total labile DOC available for microbes to respire and might correspond to light treatments in this study that increased or decreased the magnitude of microbial respiration, respectively. Consistent with the former, prior work demonstrated that a major effect of sunlight exposure of permafrost DOC was to produce DOC labile to microbial respiration (Nalven et al., 2020; Ward et al., 2017). Results from this study suggest that the labile DOC produced by sunlight is relatively younger than the DOC respired by microbes in the dark.

These results confirming microbial respiration of old permafrost DOC both in the dark and after light exposure should apply to permafrost-thaw impacted waters across the Arctic for the following reasons. First, the composition of the DOC from permafrost soils in this study, as given by $SUVA_{254}$ and fluorescence index, is within the range previously reported for permafrost organic carbon from other arctic sites (Bowen et al., 2020b; Cory et al., 2013; Mann et al., 2015; Spencer et al., 2015; Stubbins et al., 2017). Second, the ^{13}C and ^{14}C of the permafrost DOC is within the range for soil organic carbon in general (Hoefs, 2015; Trumbore & Druffel, 1995) and specifically for permafrost DOC (Bowen et al., 2020b; Mann et al., 2015; Rogers et al., 2021; Spencer et al., 2015; Stubbins et al., 2017; Vonk et al., 2013). Third, the respiratory quotients for permafrost DOC are within the range previously reported (Berggren et al., 2012; Cory et al., 2014), suggesting that microbes in this study respired terrestrially-derived DOC by similar respiratory pathways as in other freshwaters.

While the age and composition of the bulk, permafrost DOC is consistent with prior work, the age and composition of the DOC respired both in the dark and after light exposure differs from prior work. For example, prior studies showed that microbes respire fractions of permafrost DOC that are similar in both age and ^{13}C composition to the bulk DOC ($\delta^{13}C$ of respired DOC of −26 to −23‰; Mann et al., 2015; Melchert et al., 2022). In contrast, results from this study show that the CO_2 from respiration is often older and substantially more ^{13}C-depleted (−44.9‰ to −28.1‰) than the bulk DOC.

Differences in the incubation conditions and amount of DOC consumed might explain why respiration of relatively old and ^{13}C-depleted permafrost DOC fractions was observed here but not in prior studies. In prior work performed at 20°C, between 35% and 50% of permafrost DOC was respired during incubations (Mann et al., 2015; Rogers et al., 2021; Spencer et al., 2015; Vonk et al., 2013). In contrast, in this study, incubations were performed at 10°C to be representative of temperatures in arctic surface waters (Adams et al., 2010; Cory et al., 2014; Docherty et al., 2019), and respiration consumed only 1%–5% of the DOC. The lower respiration rates produced by the relatively cold incubation temperature in this study are likely more representative of respiration rates in arctic surface waters (O'Donnell et al., 2016), in comparison to incubations at higher temperatures. As the amount of DOC consumed increases, the isotopic signature of the DOC consumed becomes closer to the isotopic signature of the bulk DOC. Conversely, when only small amounts of the total DOC are consumed, there might be selective respiration of isotopically lighter fractions of the DOC pool. Thus, the C isotopic composition of CO_2 from respiration in this study might reflect the C isotopic composition of the most labile fractions of the DOC pool. However, the age and ^{13}C composition of the CO_2 from respiration is insufficient on its own to interpret the DOC substrates most labile to microbes. Thus, here we interpret the C isotopic composition of CO_2 from respiration alongside other proxies for substrate composition from this study and the literature.

4.1. Microbes Respire ^{13}C-Depleted Fractions of Permafrost DOC to CO_2

In this study, the $\delta^{13}C$ of CO_2 (Figure 2b) likely reflects the selective respiration of a range of ^{13}C-depleted fractions within the bulk DOC from each soil site. For example, microbial respiration of wet sedge and tussock tundra A DOC produced CO_2 that was highly ^{13}C-depleted relative to the expected range of $\delta^{13}C$ for bulk soil organic carbon (Drake et al., 2015; Hoefs, 2015; Mann et al., 2015; Melchert et al., 2022; Trumbore & Druffel, 1995). Microbial respiration of predominantly lipid or lignin-like fractions of the DOC pool could produce ^{13}C-depleted CO_2 because these compound classes are more depleted in ^{13}C compared to other fractions of DOC ($\delta^{13}C$ ranges of −27 to −38‰ for lipids and −25 to −32‰ for lignin-like DOC; Benner et al., 1987;

Bertoldi et al., 2014; Kling & Fry, 1992; McCallister & del Giorgio, 2008). From other soil sites (tussock tundra B and thermokarst), microbial respiration produced CO_2 that, while still ^{13}C-depleted relative to the DOC, was much closer to the ^{13}C composition of the bulk DOC. At these sites, microbes might have respired a range of the fractions of the DOC pool, including relatively ^{13}C-depleted lipid and lignin-like compounds as well as relatively ^{13}C-enriched carbohydrates and organic acids (Bowling et al., 2008; Whelan et al., 1970). In addition to preferential microbial respiration of ^{13}C-depleted sources within the DOC pool, other processes might have contributed to the respiration of a range of ^{13}C-depleted CO_2 (Section S2.2 in Supporting Information S1).

The respiratory quotient of CO_2 production to O_2 consumption during respiration provides further evidence in support of microbial respiration of a range of fractions of DOC (Figure 3a). The range of respiratory quotients for respiration of DOC in the literature (~0.5–4; Allesson et al., 2016; Berggren et al., 2012; Cory et al., 2014; del Giorgio et al., 2006) is hypothesized to depend on the composition of the DOC compounds respired (Masiello et al., 2008). Relatively more reduced (and relatively ^{13}C-depleted) lipid and lignin-like compounds are predicted to be respired with a lower respiratory quotient than are more oxidized (and relatively ^{13}C-enriched) carbohydrates and organic acids within the DOC pool (Dilly, 2001; Masiello et al., 2008; Romero-Kutzner et al., 2015). Assuming the hypothesis above explains variability in the respiratory quotient for DOC, then the strong, positive correlation between the respiratory quotient and the ^{13}C of the CO_2 from respiration (Figure 3a) is consistent with the expected ^{13}C composition of different fractions of the DOC pool.

Results in this study suggesting that old, ^{13}C-depleted DOC can constitute the majority of the DOC respired by microbes from the wet sedge and tussock tundra A permafrost soil sites are consistent with prior work. Rogers et al. (2021) provided evidence that the oldest, most ^{13}C-depleted fractions of DOC from Yedoma permafrost soil separate out at the lowest energies by ramped-pyrolysis oxidation and thus might be the most labile to microbial respiration (Leifeld & von Lützow, 2014), as observed for the wet sedge and tussock tundra A permafrost soils in this study (Figure 3b).

There are also several lines of evidence from prior work for respiration of lignin-like permafrost DOC, which is proposed to contribute to the highly ^{13}C-depleted signature of the most labile permafrost DOC in this study. For example, lignin-like formulas constituted a substantial percentage of the DOC respired by microbes from permafrost soils in previous studies (Nalven et al., 2020; Rogers et al., 2021; Ward et al., 2017). Additionally, microbial communities associated with permafrost soils across the Arctic have been shown to have a relatively high abundance of genes related to the metabolism of a wide range of organic carbon fractions including aromatic DOC associated with lignin (Nalven et al., 2020; Waldrop et al., 2023). These findings suggest that permafrost microbial communities are equipped to respire the abundant lignin-like fractions of the DOC pool (Ward et al., 2017).

Unlike lignin-like DOC, lipid fractions have not been shown to be consumed by microbes from permafrost DOC. However, lipid fractions of soil organic matter are relatively labile to microbial respiration (e.g., Reynolds et al., 2018). The lack of evidence for respiration of lipid fractions of permafrost DOC could be due to limitations of the electrospray ionization (ESI) FT-ICR MS analysis that has frequently been used to characterize the composition of DOC (Rogers et al., 2021; Spencer et al., 2015; Ward et al., 2017). Lipid fractions of DOC are known to ionize poorly via ESI, making it difficult to assess changes in the lipid content of permafrost DOC (Hockaday et al., 2009).

4.2. Light Exposure Had Wavelength-Dependent Effects on the Magnitude of DOC Respired

Given that the most common effect of light treatment was to increase respiration relative to respiration in the dark (Figure 1, Figure S3 and Table S4 in Supporting Information S1), results from this study are generally consistent with the prior conclusion that exposure of permafrost DOC to broadband sunlight stimulates microbial respiration (Cory et al., 2013; Nalven et al., 2020; Ward et al., 2017). However, results from this study show that different wavelengths of light have a broader range of effects on respiration than previously observed, ranging from increasing to decreasing respiration relative to respiration of DOC kept in the dark. These effects are likely due to changes in the DOC pool size and the DOC chemical composition.

Light exposure of DOC has been proposed to increase or decrease respiration by increasing or decreasing the amount of DOC labile to microbes, respectively (Bowen et al., 2020a; Ward et al., 2017; Wetzel et al., 1995). Light exposure of DOC can change the amount of biologically labile DOC by completely oxidizing some of this

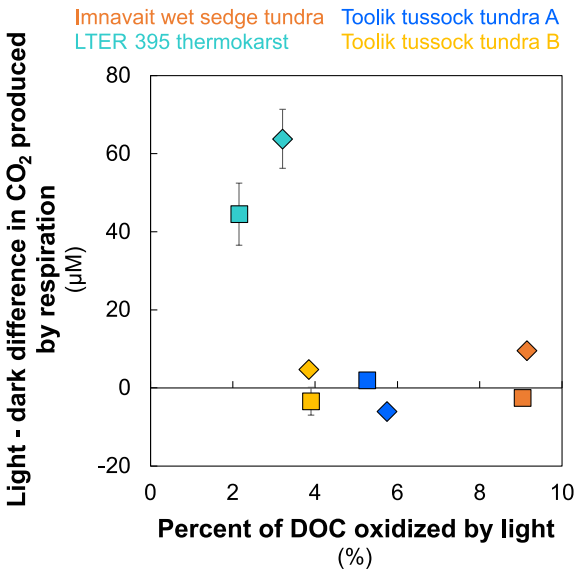

Figure 4. The difference between CO_2 production from microbial respiration in light and dark DOC treatments versus the percentage of DOC that was oxidized by light prior to biological incubations for DOC exposed to ultraviolet light (UV; 305 nm, diamond symbols) and visible light (405 nm, square symbols). Values for the difference between CO_2 production from respiration in light and dark DOC treatments are shown as the average ±1 SE of experimental replicates ($n = 3$).

DOC to CO_2 (reducing the total amount of DOC labile to respiration), and by concurrently changing the chemical composition of the remaining DOC to make it more or less labile to microbes (Bowen et al., 2020a; Cory et al., 2010; Ward & Cory, 2016; Wetzel et al., 1995; Xie et al., 2004). Therefore, changes in the magnitude of respiration after DOC light exposure reflect the net effect of light exposure on the size of the labile DOC pool.

The net effect of light exposure on the amount of labile DOC—and, thus, on whether respiration increases or decreases after light exposure relative to respiration of dark DOC—likely depends on the extent to which DOC was oxidized during light exposure in this study. For the two soil sites with less than 5% of the DOC pool oxidized to CO_2 by UV or visible light (tussock tundra B and thermokarst; Figure 4), both UV and visible light had either no net effect or increased respiration relative to respiration in the dark. For the two soil sites where 5% or more of the DOC pool was oxidized to CO_2 by UV or visible light (wet sedge and tussock tundra A), UV and visible light either increased or decreased respiration relative to respiration in the dark (Figure 4). These results are consistent with prior work demonstrating that increasing oxidation of DOC by broadband sunlight generally increases respiration when a relatively small amount (<5%) of the DOC is oxidized to CO_2 (Bowen et al., 2020a; Reader & Miller, 2014; Ward et al., 2017) but might have diminishing returns or even decrease respiration relative to respiration in the dark at greater amounts of DOC oxidized (Bowen et al., 2020a; Reader & Miller, 2014).

For DOC from a given soil site, UV and visible light doses were chosen to achieve the same extent of DOC oxidation by light of both wavelengths (Table S3 in Supporting Information S1). Thus, the differences in the microbial response to UV versus visible light-exposed DOC for a given soil site should be due to wavelength-dependent differences in the production and removal of labile DOC. UV wavelengths of light have been proposed to be more efficient at yielding low molecular weight acids and aldehydes than are visible wavelengths of light (Miller et al., 2002; Wetzel et al., 1995). In turn, low molecular weight acid and aldehyde photo-products are thought to be highly biologically labile (Drake et al., 2015; Miller et al., 2002) and might account for increases in respiration after light exposure of DOC. For the wet sedge and thermokarst soil sites, for which UV light exposure of DOC increased respiration (Figure 1, Table S4 in Supporting Information S1), the relatively high respiratory quotients for DOC exposed to UV light (≥1) are consistent with respiration of organic acids (Table S4 in Supporting Information S1; Masiello et al., 2008). For the UV light treatment of the thermokarst site, production of CO_2 with a ^{13}C composition similar to the bulk DOC provides further evidence in support of respiration of organic acids, which are expected to have a similar ^{13}C composition to that of the bulk DOC (Figure 2b, Table 1; Bowling et al., 2008). These results suggest that UV light was relatively more efficient at producing labile DOC than was visible light for DOC from the wet sedge and thermokarst soils.

However, higher-energy UV light might also be relatively more efficient at removing biologically labile DOC than is lower-energy visible light (Reader & Miller, 2014). When this is the case, net production of labile DOC might be higher under visible light than UV light. For example, for the tussock tundra A soil site, UV light decreased respiration while visible light increased respiration relative to respiration in the dark (Figure 1, Figure S3 and Table S4 in Supporting Information S1). For this soil site, the relatively high respiratory quotient for DOC exposed to visible light (RQ of 0.96; Figure S3 and Table S4 in Supporting Information S1), compared to the relatively lower respiratory quotient for DOC from the same site exposed to UV light, is consistent with respiration of labile organic acids (Masiello et al., 2008) following exposure of DOC to visible light.

However, there are conflicting conclusions in the literature about whether changes in DOC composition during light exposure could affect the respiratory quotient. Some studies report increases in the respiratory quotient after light exposure, interpreted as respiration of more highly oxidized, low molecular weight DOC photoproducts from light-exposed DOC than from dark DOC (Allesson et al., 2016; Berggren et al., 2012). In contrast, other studies provide evidence that microbes respire the same types of DOC after light exposure that they are already

genomically-equipped to respire in the dark (Cory et al., 2014; Nalven et al., 2020; Ward et al., 2017). Results of this study provide support for the latter interpretation by demonstrating that microbes respired fractions of the DOC pool with similar ^{13}C compositions and respiratory quotients both after light exposure and in the dark for DOC from most soils and wavelengths of light (Figure 2b, Figure S3 and Table S4 in Supporting Information S1). Given that both the $\delta^{13}C$ of CO_2 from respiration and the respiratory quotient are thought to depend on the composition of the DOC (Berggren et al., 2012; Crow et al., 2006; Masiello et al., 2008; Pries et al., 2020), these results suggest that light exposure of DOC did not substantially change the fractions of DOC respired or their respiratory pathways compared to respiratory pathways in the dark for most soil sites. Thus, changes in the magnitude of respiration after light exposure are most likely a response to changes in the size of the labile DOC pool, rather than to major shifts in the composition of the most labile DOC available to microbes.

4.3. Rates of Microbial Respiration of Permafrost DOC in Arctic Surface Waters

Water-column production rates for any product of DOC photodegradation are sensitive to the wavelength-dependent yield of the product per mole of light absorbed by chromophoric dissolved organic matter (CDOM, the light-absorbing fraction of DOC). In the case of respiration increased or decreased by DOC light exposure, the product is more or less CO_2 from respiration upon absorption of light by CDOM, respectively, compared to respiration in the dark. In prior studies where exposure of DOC to broadband (natural) sunlight was found to increase respiration of the DOC relative to dark controls (Cory et al., 2013, 2014), the assumptions were that (a) all wavelengths of sunlight increased respiration of DOC, and (b) exposure of DOC to UV wavelengths of sunlight was more efficient at increasing respiration than exposure to visible wavelengths of sunlight (e.g., Cory et al., 2013, 2014). In contrast, this study shows that both UV and visible wavelengths of light can also decrease respiration relative to respiration in the dark. Additionally, this study shows that exposure to UV light can result in similar or lower amounts of CO_2 from respiration than does exposure to visible light for some permafrost DOC. Thus, water-column rates of respiration of sunlight-exposed DOC (e.g., Cory et al., 2014) must be revised in response to the invalidated assumptions.

A quantitative revision of water-column rates of respiration of sunlight-exposed DOC requires measurements of the wavelength-dependent yield of more or less CO_2 from respiration per mole of light absorbed by CDOM, which was not possible based on the experimental design in this study (see Section S1.3 in Supporting Information S1). However, results from this study enable a qualitative assessment of the net effect of sunlight exposure of DOC on water-column respiration rates. An important factor modulating the wavelength-dependent effect of DOC light exposure on water column respiration rates is the amount of UV versus visible light absorbed by DOC in the water column. Although absorbance of light by DOC is much higher in the UV than in the visible, more total visible than UV light reaches the surface, and thus more visible than UV light is absorbed by DOC in the water column (Figure S5 in Supporting Information S1). Thus, relatively small yields of more or less CO_2 from respiration of DOC exposed to visible light can have a disproportionately large impact on water-column rates of CO_2 production compared to the yields of CO_2 from respiration of DOC exposed to UV light.

For example, for the tussock tundra A DOC, the extra CO_2 from respiration of tussock tundra DOC exposed to visible light might completely or partially offset the reduction in CO_2 from respiration of tussock tundra DOC exposed to UV wavelengths of light, relative to respiration in the dark. Conversely, for wet sedge DOC, the reduction in CO_2 from respiration of wet sedge DOC exposed to visible wavelengths of light might completely or partially offset the extra CO_2 from respiration of wet sedge DOC exposed to UV wavelengths of light.

However, the experimental light doses in this study were chosen to achieve equal oxidation of DOC by both UV and visible wavelengths of light for each soil site (Table S3 in Supporting Information S1) and are not representative of the ratio of UV to visible photon doses reaching arctic surface waters. To oxidize the same amount of DOC with visible as with UV light, the ratio of visible to UV light received by DOC from LEDs in this study (~56:1; Table S3 in Supporting Information S1) was ~5 times greater than the ratio of visible to UV light received by DOC from natural sunlight in arctic surface waters (~11:1; Bowen et al., 2020b). This difference in the ratio of visible to UV between this study and broadband sunlight in prior work might explain why prior work has reported that sunlight generally increases microbial respiration relative to respiration in the dark (Cory et al., 2013, 2014; Ward et al., 2017). For example, consider the DOC from the wet sedge soil site, for which this study showed that UV light exposure increases respiration and visible light exposure decreases respiration relative to respiration in the dark (Table S4 in Supporting Information S1). In arctic surface waters, wet sedge DOC would receive ~5

times less visible light than in this study over the period of time required to receive the same amount of UV light as in this study. As discussed previously, small doses of light frequently increase microbial respiration relative to respiration in the dark, while larger doses of light can decrease microbial respiration because labile DOC is increasingly altered or removed during photo-oxidation. Therefore, while this study showed that relatively large doses of visible light decrease respiration of wet sedge DOC, it is possible that the lower doses of visible light from natural sunlight would have a weaker effect.

These results demonstrate two knowledge gaps to be addressed to quantify water-column rates of CO_2 production from respiration of DOC in sunlit surface waters. First, the wavelength dependence of the yield of more or less CO_2 from respiration of sunlight-exposed DOC must be quantified. Second, the wavelength-dependent yield of any product of DOC photodegradation (including CO_2 from respiration) should be quantified using doses of UV and visible light similar to what is absorbed by DOC during its residence times in sunlit surface waters.

5. Conclusions

By measuring the age of CO_2 produced by respiration of light-exposed permafrost DOC, we show that ancient permafrost DOC is respired upon exposure to sunlight in arctic surface waters. The CO_2 produced by microbes in light treatments and in dark controls was as old or older than the bulk DOC. It is already established that the coupled oxidation by sunlight and microbial respiration of DOC is an important control on the oxidation of modern DOC to CO_2 in arctic surface waters (Cory et al., 2013, 2014; Stubbins et al., 2017; Ward et al., 2017). As the annual thaw depth increases, or as thermokarst failures expose permafrost soils to surface conditions, the modern DOC exported from land to water will be increasingly mixed with old organic compounds ranging in age from a few thousands of years up to ~45,000 years before present (Schwab et al., 2020; Strauss et al., 2017). Therefore, sunlight exposure will continue to be an important control on the magnitude of CO_2 emitted from arctic freshwaters as the DOC in these waters is increasingly comprised of ancient permafrost carbon in a warming Arctic.

Additionally, this study showed that the permafrost DOC respired by microbes both in the dark and after light exposure was substantially ^{13}C-depleted relative to the bulk DOC. This result is interpreted as evidence that ^{13}C-depleted fractions of the permafrost DOC pool, including a mixture of lipid and lignin-like DOC, are more biologically labile than ^{13}C-enriched DOC fractions, both when freshly thawed from dark soil and after exposure to sunlight. Microbial respiration of permafrost DOC in small headwater streams that are most strongly impacted by permafrost thaw (Aiken et al., 2014; Neff et al., 2006; Vonk et al., 2013) is likely fueled primarily by these most labile, ^{13}C-depleted fractions of the permafrost DOC pool. In these waters, labile permafrost DOC that is consumed by coupled oxidation by sunlight and microbial respiration is expected to be rapidly replenished by fresh DOC inputs from soils (Cory et al., 2015; Neilson et al., 2018). However, as water residence times increase, the DOC remaining that is exported downstream might be composed of a greater percentage of ^{13}C-enriched fractions than DOC received from permafrost soils.

Results of this study and prior work (Bowen et al., 2020a; Cory et al., 2013; Ward et al., 2017) suggest that the magnitude of permafrost DOC respired in sunlit arctic surface waters depends in part on the extent to which DOC oxidation by sunlight changes the amount of labile DOC. Sunlight exposure is expected to consistently increase respiration of permafrost DOC (relative to respiration in the dark) in arctic headwater streams, where short residence times of days to weeks mean that a small percentage of permafrost DOC will be oxidized by sunlight prior to export downstream (Cory et al., 2015). As permafrost DOC moves from headwater streams to larger streams, both the water residence time and stream surface area increase (e.g., Neilson et al., 2018). With increasing time spent in sunlit waters, the percentage of permafrost DOC oxidized by both sunlight and microbes in larger streams is generally expected to increase (Cory et al., 2015). Greater oxidation of DOC by sunlight in larger streams might increasingly remove DOC labile to microbes, offsetting some of the increases in oxidation of DOC driven by the longer water residence time. However, the reported lack of old permafrost DOC in major arctic rivers (Aiken et al., 2014; Neff et al., 2006; Rogers et al., 2021; Vonk et al., 2013; Wild et al., 2019) suggests that more of the permafrost DOC reaching surface waters is oxidized to CO_2 than is exported downstream to larger rivers. Results from this study implicate increased respiration of sunlight-exposed DOC as a contributor to this loss of permafrost DOC in the smaller, shallow, unshaded surface waters of the Arctic (Cory et al., 2014) that are increasingly ice-free during peak solar radiation (Cooley et al., 2019; Zhang et al., 2021).

Conflict of Interest

The authors declare no conflicts of interest relevant to this study.

Data Availability Statement

All data are available in the manuscript or the Supporting Information S1, and data are available at the Arctic LTER (https://arc-lter.ecosystems.mbl.edu/arctic-data-catalog) (Cory et al., 2023a, 2023b, 2023c, 2023d, 2023e).

Acknowledgments
We thank K. Clippinger, N. LaFramboise, J. Bowen, J. Dobkowski, K. Romanowicz, N. Christman, B. Crump, E. Peterson, and researchers, technicians, and support staff of the Arctic LTER and Toolik Field Station for assistance with field and laboratory work. We additionally thank K. Romanowicz for providing methane concentrations for permafrost soil leachates. We thank J. Burton, L. Xu, and researchers and technicians at the National Ocean Sciences AMS (NOSAMS) facility at WHOI for training and assistance with carbon isotope measurements. Research was supported by NSF DDRIG 2228992 (R.M.C. and E.C.R.), NSF DEB 1754835 and 2224743 (G.W.K. and R.M.C.), NSF DEB 1637459 and OPP 1936769 (G.W.K), and NSF OCE 2219660 (C.P.W.). All authors contributed to the study design, sample collection, laboratory experiments, data analysis, and manuscript preparation.

References

Abbott, B. W., Larouche, J. R., Jones, J. B., Bowden, W. B., & Balser, A. W. (2014). Elevated dissolved organic carbon biodegradability from thawing and collapsing permafrost. *Journal of Geophysical Research: Biogeosciences*, *119*(10), 2049–2063. https://doi.org/10.1002/2014JG002678

Adams, H. E., Crump, B. C., & Kling, G. W. (2010). Temperature controls on aquatic bacterial production and community dynamics in arctic lakes and streams. *Environmental Microbiology*, *12*(5), 1319–1333. https://doi.org/10.1111/j.1462-2920.2010.02176.x

Aiken, G. R., Spencer, R. G. M., Striegl, R. G., Schuster, P. F., & Raymond, P. A. (2014). Influences of glacier melt and permafrost thaw on the age of dissolved organic carbon in the Yukon River basin. *Global Biogeochemical Cycles*, *28*(5), 525–537. https://doi.org/10.1002/2013GB004764

Allesson, L., Ström, L., & Berggren, M. (2016). Impact of photochemical processing of DOC on the bacterioplankton respiratory quotient in aquatic ecosystems. *Geophysical Research Letters*, *43*(14), 7538–7545. https://doi.org/10.1002/2016GL069621

Andrews, S. S., Caron, S., & Zafiriou, O. C. (2000). Photochemical oxygen consumption in marine waters: A major sink for colored dissolved organic matter? *Limnology & Oceanography*, *45*(2), 267–277. https://doi.org/10.4319/lo.2000.45.2.0267

Beaupré, S. R., & Druffel, E. R. M. (2012). Photochemical reactivity of ancient marine dissolved organic carbon. *Geophysical Research Letters*, *39*(18), L18602. https://doi.org/10.1029/2012GL052974

Beaupré, S. R., Druffel, E. R. M., & Griffin, S. (2007). A low-blank photochemical extraction system for concentration and isotopic analyses of marine dissolved organic carbon. *Limnology and Oceanography: Methods*, *5*(6), 174–184. https://doi.org/10.4319/lom.2007.5.174

Benner, R., Fogel, M. L., Sprague, E. K., & Hodson, R. E. (1987). Depletion of ^{13}C in lignin and its implications for stable carbon isotope studies. *Nature*, *329*(6141), 708–710. https://doi.org/10.1038/329708a0

Berggren, M., Lapierre, J. F., & del Giorgio, P. A. (2012). Magnitude and regulation of bacterioplankton respiratory quotient across freshwater environmental gradients. *The ISME Journal*, *6*(5), 984–993. https://doi.org/10.1038/ismej.2011.157

Bertoldi, D., Santato, A., Paolini, M., Barbero, A., Camin, F., Nicolini, G., & Larcher, R. (2014). Botanical traceability of commercial tannins using the mineral profile and stable isotopes. *Journal of Mass Spectrometry*, *49*(9), 792–801. https://doi.org/10.1002/jms.3457

Bowen, J. C., Kaplan, L. A., & Cory, R. M. (2020a). Photodegradation disproportionately impacts biodegradation of semi-labile DOM in streams. *Limnology & Oceanography*, *65*(1), 13–26. https://doi.org/10.1002/lno.11244

Bowen, J. C., Ward, C. P., Kling, G. W., & Cory, R. M. (2020b). Arctic amplification of global warming strengthened by sunlight oxidation of permafrost carbon to CO_2. *Geophysical Research Letters*, *47*(12), 0–3. https://doi.org/10.1029/2020GL087085

Bowling, D. R., Pataki, D. E., & Randerson, J. T. (2008). Carbon isotopes in terrestrial ecosystem pools and CO_2 fluxes. *New Phytologist*, *178*(1), 24–40. https://doi.org/10.1111/j.1469-8137.2007.02342.x

Cooley, S. W., Smith, L. C., Ryan, J. C., Pitcher, L. H., & Pavelsky, T. M. (2019). Arctic-Boreal lake dynamics revealed using CubeSat imagery. *Geophysical Research Letters*, *46*(4), 2111–2120. https://doi.org/10.1029/2018GL081584

Cory, R. M., Crump, B. C., Dobkowski, J. A., & Kling, G. W. (2013). Surface exposure to sunlight stimulates CO_2 release from permafrost soil carbon in the Arctic. *Proceedings of the National Academy of Sciences of the United States of America*, *110*(9), 3429–3434. https://doi.org/10.1073/pnas.1214104110

Cory, R. M., Harrold, K. H., Neilson, B. T., & Kling, G. W. (2015). Controls on dissolved organic matter (DOM) degradation in a headwater stream: The influence of photochemical and hydrological conditions in determining light-limitation or substrate-limitation of photo-degradation. *Biogeosciences*, *12*(22), 6669–6685. https://doi.org/10.5194/bg-12-6669-2015

Cory, R. M., & Kaplan, L. A. (2012). Biological lability of streamwater fluorescent dissolved organic matter. *Limnology & Oceanography*, *57*(5), 1347–1360. https://doi.org/10.4319/lo.2012.57.5.1347

Cory, R. M., & Kling, G. W. (2018). Interactions between sunlight and microorganisms influence dissolved organic matter degradation along the aquatic continuum. *Limnology and Oceanography Letters*, *3*(3), 102–116. https://doi.org/10.1002/lol2.10060

Cory, R. M., McNeill, K., Cotner, J. P., Amado, A., Purcell, J. M., & Marshall, A. G. (2010). Singlet oxygen in the coupled photochemical and biochemical oxidation of dissolved organic matter. *Environmental Science & Technology*, *44*(10), 3683–3689. https://doi.org/10.1021/es902989y

Cory, R. M., Rieb, E. C., Polik, C. A., Ward, C. P., & Kling, G. W. (2023a). Accession numbers for radiocarbon and stable carbon isotopes of dissolved organic carbon (DOC) and dissolved inorganic carbon (DIC) in soil leachates from permafrost soils collected from the North Slope of Alaska in the summers of 2018 and 2022 (Version 1) [Dataset]. *Environmental Data Initiative*. https://doi.org/10.6073/pasta/f7a565d6b8b8ca1b5fa2d8f4d28dee4b

Cory, R. M., Rieb, E. C., Polik, C. A., Ward, C. P., & Kling, G. W. (2023b). Daily water-column rates of sunlight absorption by chromophoric dissolved organic matter (CDOM) leached from permafrost soils collected from the North Slope of Alaska in the summers of 2018 and 2022 (Version 1) [Dataset]. *Environmental Data Initiative*. https://doi.org/10.6073/pasta/3a34daab0f8bb4e59ef39068f311fa94

Cory, R. M., Rieb, E. C., Polik, C. A., Ward, C. P., & Kling, G. W. (2023c). Methane concentrations in dissolved organic carbon (DOC) leachates from permafrost soils collected from the North Slope of Alaska in the summers of 2018 and 2019 (Version 1) [Dataset]. *Environmental Data Initiative*. https://doi.org/10.6073/pasta/e386e272d73577e42b2ae1a18fecf6a0

Cory, R. M., Rieb, E. C., Polik, C. A., Ward, C. P., & Kling, G. W. (2023d). Preparation of dissolved organic carbon (DOC) leachates from permafrost soils collected from the North Slope of Alaska in the summers of 2018 and 2022 (Version 1) [Dataset]. *Environmental Data Initiative*. https://doi.org/10.6073/pasta/1bf2a9fcbd47f8af1c789cabe02322d6

Cory, R. M., Rieb, E. C., Polik, C. A., Ward, C. P., & Kling, G. W. (2023e). Radiocarbon and stable carbon isotopes of carbon dioxide produced by respiration of dissolved organic carbon (DOC) leached from permafrost soils collected from the North Slope of Alaska in the summers of 2018 and 2022 (Version 1) [Dataset]. *Environmental Data Initiative*. https://doi.org/10.6073/pasta/50e5f1dbff90130bd40658e9f00a14d3

Cory, R. M., Ward, C. P., Crump, B. C., & Kling, G. W. (2014). Sunlight controls water column processing of carbon in arctic fresh waters. *Science*, *345*(6199), 925–928. https://doi.org/10.1126/science.1253119

Crow, S. E., Sulzman, E. W., Rugh, W. D., Bowden, R. D., & Lajtha, K. (2006). Isotopic analysis of respired CO_2 during decomposition of separated soil organic matter pools. *Soil Biology and Biochemistry*, *38*(11), 3279–3291. https://doi.org/10.1016/j.soilbio.2006.04.007

Del Giorgio, P. A., Pace, M. L., & Fischer, D. (2006). Relationship of bacterial growth efficiency to spatial variation in bacterial activity in the Hudson River. *Aquatic Microbial Ecology*, *45*(1), 55–67. https://doi.org/10.3354/ame045055

Dilly, O. (2001). Microbial respiratory quotient during basal metabolism and after glucose amendment in soils and litter. *Soil Biology and Biochemistry*, *33*(1), 117–127. https://doi.org/10.1016/S0038-0717(00)00123-1

Docherty, C. L., Dugdale, S. J., Milner, A. M., Abermann, J., Lund, M., & Hannah, D. M. (2019). Arctic river temperature dynamics in a changing climate. *River Research and Applications*, *35*(8), 1212–1227. https://doi.org/10.1002/rra.3537

Drake, T. W., Wickland, K. P., Spencer, R. G. M., & Striegl, R. G. (2015). Ancient low-molecular-weight organic acids in permafrost fuel rapid carbon dioxide production upon thaw. *Proceedings of the National Academy of Sciences of the United States of America*, *112*(45), 13946–-13951. https://doi.org/10.1073/pnas.1511705112

Frey, K. E., & McClelland, J. W. (2009). Impacts of permafrost degradation on arctic river biogeochemistry. *Hydrological Processes*, *23*(1), 169–182. https://doi.org/10.1002/hyp.7196

Hamilton, T. D. (2003). Glacial geology of the Toolik Lake and Upper Kuparuk River Regions. In *Biological papers of the University of Alaska* (pp. 1–24). University of Alaska.

Hockaday, W. C., Purcell, J. M., Marshall, A. G., Baldock, J. A., & Hatcher, P. G. (2009). Electrospray and photoionization mass spectrometry for the characterization of organic matter in natural waters: A qualitative assessment. *Limnology and Oceanography: Methods*, *7*(1), 81–95. https://doi.org/10.4319/lom.2009.7.81

Hoefs, J. (2015). *Stable isotope geochemistry* (6th ed.). Springer-Verlag. https://doi.org/10.1007/978-3-540-70708-0

Ishikawa, N. F., Butman, D., & Raymond, P. A. (2019). Radiocarbon age of different photoreactive fractions of freshwater dissolved organic matter. *Organic Geochemistry*, *135*, 11–15. https://doi.org/10.1016/j.orggeochem.2019.06.006

Jorgenson, M. T., Shur, Y. L., & Pullman, E. R. (2006). Abrupt increase in permafrost degradation in Arctic Alaska. *Geophysical Research Letters*, *33*(2), L02503. https://doi.org/10.1029/2005GL024960

Kling, G. W., Fry, B., & O'Brien, W. J. (1992). Stable isotopes and planktonic trophic structure in Arctic Lakes. *Ecology*, *73*(2), 561–566. https://doi.org/10.2307/1940762

Kling, G. W., Kipphut, G. W., Miller, M. M., & O'Brien, W. J. (2000). Integration of lakes and streams in a landscape perspective: The importance of material processing on spatial patterns and temporal coherence. *Freshwater Biology*, *43*(4), 477–497. https://doi.org/10.1046/j.1365-2427.2000.00515.x

Kokelj, S. V., & Jorgenson, M. T. (2013). Advances in Thermokarst Research. *Permafrost and Periglacial Processes*, *24*(2), 108–119. https://doi.org/10.1002/ppp.1779

Leifeld, J., & von Lützow, M. (2014). Chemical and microbial activation energies of soil organic matter decomposition. *Biology and Fertility of Soils*, *50*(1), 147–153. https://doi.org/10.1007/s00374-013-0822-6

Li, A., Aubeneau, A. F., King, T., Cory, R. M., Neison, B. T., Bolster, D., & Packman, A. I. (2019). Effects of vertical hydrodynamic mixing on photomineralization of dissolved organic carbon in arctic surface waters. *Environmental Sciences: Processes & Impacts*, *21*(4), 748–760. https://doi.org/10.1039/C8EM00455B

Longworth, B. E., Von Reden, K. F., Long, P., & Roberts, M. L. (2015). A high output, large acceptance injector for the NOSAMS Tandetron AMS system. *Nuclear Instruments and Methods in Physics Research Section B: Beam Interactions with Materials and Atoms*, *361*, 211–216. https://doi.org/10.1016/j.nimb.2015.04.005

Mann, P. J., Eglinton, T. I., McIntyre, C. P., Zimov, N., Davydova, A., Vonk, J. E., et al. (2015). Utilization of ancient permafrost carbon in headwaters of Arctic fluvial networks. *Nature Communications*, *6*(1), 7856. https://doi.org/10.1038/ncomms8856

Mann, P. J., Sobczak, W. V., Larue, M. M., Bulygina, E., Davydova, A., Vonk, J. E., et al. (2014). Evidence for key enzymatic controls on metabolism of Arctic river organic matter. *Global Change Biology*, *20*(4), 1089–1100. https://doi.org/10.1111/gcb.12416

Masiello, C. A., Gallagher, M. E., Randerson, J. T., Deco, R. M., & Chadwick, O. A. (2008). Evaluating two experimental approaches for measuring ecosystem carbon oxidation state and oxidative ratio. *Journal of Geophysical Research*, *113*(G3), G03010. https://doi.org/10.1029/2007JG000534

McCallister, S. L., & del Giorgio, P. A. (2008). Direct measurement of the $\delta^{13}C$ signature of carbon respired by bacteria in lakes: Linkages to potential carbon sources, ecosystem baseline metabolism, and CO_2 fluxes. *Limnology & Oceanography*, *53*(4), 1204–1216. https://doi.org/10.4319/lo.2008.53.4.1204

McCallister, S. L., & del Giorgio, P. A. (2012). Evidence for the respiration of ancient terrestrial organic C in northern temperate lakes and streams. *Proceedings of the National Academy of Sciences of the United States of America*, *109*(42), 16963–16968. https://doi.org/10.1073/pnas.1207305109

McFarlane, K. J., Throckmorton, H. M., Heikoop, J. M., Newman, B. D., Hedgpeth, A. L., Repasch, M. N., et al. (2022). Age and chemistry of dissolved organic carbon reveal enhanced leaching of ancient labile carbon at the permafrost thaw zone. *Biogeosciences*, *19*(4), 1211–1223. https://doi.org/10.5194/bg-19-1211-2022

McGuire, A. D., Lawrence, D. M., Koven, C., Clein, J. S., Burke, E., Chen, G., et al. (2018). Dependence of the evolution of carbon dynamics in the northern permafrost region on the trajectory of climate change. *Proceedings of the National Academy of Sciences of the United States of America*, *115*(15), 3882–3887. https://doi.org/10.1073/pnas.1719903115

Melchert, J. O., Wischhöfer, P., Knoblauch, C., Eckhardt, T., Liebner, S., & Rethemeyer, J. (2022). Sources of CO_2 produced in freshly thawed pleistocene-age Yedoma permafrost. *Frontiers in Earth Science*, *9*. https://doi.org/10.3389/feart.2021.737237

Miller, W. L., Moran, M., Sheldon, W. M., Zepp, R. G., & Opsahl, S. (2002). Determination of apparent quantum yield spectra for the formation of biologically labile photoproducts. *Limnology & Oceanography*, *47*(2), 343–352. https://doi.org/10.4319/lo.2002.47.2.0343

Nalven, S. G., Ward, C. P., Payet, J. P., Cory, R. M., Kling, G. W., Sharpton, T. J., et al. (2020). Experimental metatranscriptomics reveals the costs and benefits of dissolved organic matter photo-alteration for freshwater microbes. *Environmental Microbiology*, *22*(8), 3505–3521. https://doi.org/10.1111/1462-2920.15121

Neff, J. C., Finlay, J. C., Zimov, S. A., Davydov, S. P., Carrasco, J. J., Schuur, E. A. G., & Davydova, A. I. (2006). Seasonal changes in the age and structure of dissolved organic carbon in Siberian rivers and streams. *Geophysical Research Letters*, *33*(23), L23401. https://doi.org/10.1029/2006GL028222

Neilson, B. T., Cardenas, M. B., O'Connor, M. T., Rasmussen, M. T., King, T. V., & Kling, G. W. (2018). Groundwater flow and exchange across the land surface explain carbon export patterns in continuous permafrost watersheds. *Geophysical Research Letters*, *45*(15), 7596–7605. https://doi.org/10.1029/2018GL078140

O'Donnell, J. A., Aiken, G. R., Swanson, D. K., Panda, S., Butler, K. D., & Baltensperger, A. P. (2016). Dissolved organic matter composition of Arctic rivers: Linking permafrost and parent material to riverine carbon. *Global Biogeochemical Cycles*, *30*(12), 1811–1826. https://doi.org/10.1002/2016GB005482

Olefeldt, D., Goswami, S., Grosse, G., Hayes, D., Hugelius, G., Kuhry, P., et al. (2016). Circumpolar distribution and carbon storage of thermokarst landscapes. *Nature Communications*, *7*(1), 13043. https://doi.org/10.1038/ncomms13043

Osterkamp, T. E. (2007). Characteristics of the recent warming permafrost in Alaska. *Journal of Geophysical Research*, *112*(F2), F02S02. https://doi.org/10.1029/2006JF000578

Page, S. E., Kling, G. W., Sander, M., Harrold, K. H., Logan, J. R., McNeill, K., & Cory, R. M. (2013). Dark formation of hydroxyl radical in arctic soil and surface waters. *Environmental Science & Technology*, *47*(22), 12860–12867. https://doi.org/10.1021/es4033265

Page, S. E., Logan, J. R., Cory, R. M., & McNeill, K. (2014). Evidence for dissolved organic matter as the primary source and sink of photochemically produced hydroxyl radical in arctic surface waters. *Environmental Sciences: Processes & Impacts*, *16*(4), 807–822. https://doi.org/10.1039/c3em00596h

Ping, C. L., Bockheim, J. G., Kimble, J. M., Michaelson, G. J., & Walker, D. A. (1998). Characteristics of cryogenic soils along a latitudinal transect in arctic Alaska. *Journal of Geophysical Research*, *103*(D22), 28917–28928. https://doi.org/10.1029/98JD02024

Plaza, C., Pegoraro, E., Bracho, R., Celis, G., Crummer, K. G., Hutchings, J. A., et al. (2019). Direct observation of permafrost degradation and rapid soil carbon loss in tundra. *Nature Geoscience*, *12*(8), 627–631. https://doi.org/10.1038/s41561-019-0387-6

Pries, C. H., Angert, A., Castanha, C., Hilman, B., & Torn, M. S. (2020). Using respiration quotients to track changing sources of soil respiration seasonally and with experimental warming. *Biogeosciences*, *17*(12), 3045–3055. https://doi.org/10.5194/bg-17-3045-2020

Reader, H. E., & Miller, W. L. (2014). The efficiency and spectral photon dose dependence of photochemically induced changes to the bioavailability of dissolved organic carbon. *Limnology & Oceanography*, *59*(1), 182–194. https://doi.org/10.4319/lo.2014.59.1.0182

Reynolds, L. L., Lajtha, K., Bowden, R. D., Tfaily, M. M., Johnson, B. R., & Bridgham, S. D. (2018). The path from litter to soil: Insights into soil C cycling from long-term input manipulation and high-resolution mass spectrometry. *Journal of Geophysical Research: Biogeosciences*, *123*(5), 1486–1497. https://doi.org/10.1002/2017JG004076

Rogers, J. A., Galy, V., Kellerman, A. M., Chanton, J. P., Zimov, N., & Spencer, R. G. M. (2021). Limited presence of permafrost dissolved organic matter in the Kolyma River, Siberia revealed by ramped oxidation. *Journal of Geophysical Research: Biogeosciences*, *126*(7), e2020JG005977. https://doi.org/10.1029/2020JG005977

Romanowicz, J. K., & Kling, G. W. (2022). Summer thaw duration is a strong predictor of the soil microbiome and its response to permafrost thaw in arctic tundra. *Environmental Microbiology*, *24*(12), 6220–6237. https://doi.org/10.1111/1462-2920.16218

Romero-Kutzner, V., Packard, T. T., Berdalet, E., Roy, S. O., Gagné, J. P., & Gómez, M. (2015). Respiration quotient variability: Bacterial evidence. *Marine Ecology Progress Series*, *519*, 47–59. https://doi.org/10.3354/meps11062

Schuur, E. A. G., McGuire, A. D., Schädel, C., Grosse, G., Harden, J. W., Hayes, D. J., et al. (2015). Climate change and the permafrost carbon feedback. *Nature*, *520*(7546), 171–179. https://doi.org/10.1038/nature14338

Schwab, M. L., Hilton, R. G., Raymond, P. A., Haghipour, N., Amos, E., Tank, S. E., et al. (2020). An abrupt aging of dissolved organic carbon in large arctic rivers. *Geophysical Research Letters*, *47*(23), e2020GL088823. https://doi.org/10.1029/2020GL088823

Smith, S. L., O'Neill, H. B., Isaksen, K., Noetzli, J., & Romanovsky, V. E. (2022). The changing thermal state of permafrost. *Nature Reviews Earth & Environment*, *3*(1), 10–23. https://doi.org/10.1038/s43017-021-00240-1

Spencer, R. G. M., Mann, P. J., Dittmar, T., Eglinton, T. I., McIntyre, C., Holmes, R. M., et al. (2015). Detecting the signature of permafrost thaw in Arctic rivers. *Geophysical Research Letters*, *42*(8), 2830–2835. https://doi.org/10.1002/2015GL063498

Strauss, J., Schirrmeister, L., Grosse, G., Fortier, D., Hugelius, G., Knoblauch, C., et al. (2017). Deep Yedoma permafrost: A synthesis of depositional characteristics and carbon vulnerability. *Earth-Science Reviews*, *172*, 75–86. https://doi.org/10.1016/j.earscirev.2017.07.007

Stubbins, A., Mann, P. J., Powers, L., Bittar, T. B., Dittmar, T., McIntyre, C. P., et al. (2017). Low photolability of Yedoma permafrost dissolved organic carbon. *Journal of Geophysical Research: Biogeosciences*, *122*(1), 200–211. https://doi.org/10.1002/2016JG003688

Theenhaus, A., Maraun, M., & Scheu, S. (1997). Substrate-induced respiration in forest and arable soils measured by O_2-microcompensation: Moisture conditions and respiratory quotient. *Pedobiologia*, *41*(5), 449–455. https://doi.org/10.1016/s0031-4056(24)00315-9

Trumbore, S. E., & Druffel, E. R. M. (1995). Carbon isotopes for characterizing sources and turnover of nonliving organic matter. In R. G. Zepp & C. Sonntag (Eds.), *Role of nonliving organic matter in the Earth's carbon cycle* (pp. 7–22). John Wiley.

Trusiak, A., Treibergs, L. A., Kling, G. W., & Cory, R. M. (2018a). The controls of iron and oxygen on hydroxyl radical (•OH) production in soils. *Soil Systems*, *3*(1), 1. https://doi.org/10.3390/soilsystems3010001

Trusiak, A., Treibergs, L. A., Kling, G. W., & Cory, R. M. (2018b). The role of iron and reactive oxygen species in the production of CO_2 in arctic soil waters. *Geochimica et Cosmochimica Acta*, *224*, 80–95. https://doi.org/10.1016/j.gca.2017.12.022

Vaughn, L. J. S., & Torn, M. S. (2019). ^{14}C evidence that millennial and fast-cycling soil carbon are equally sensitive to warming. *Nature Climate Change*, *9*(6), 467–471. https://doi.org/10.1038/s41558-019-0468-y

Vonk, J. E., Mann, P. J., Davydov, S., Davydova, A., Spencer, R. G. M., Schade, J., et al. (2013). High biolability of ancient permafrost carbon upon thaw. *Geophysical Research Letters*, *40*(11), 2689–2693. https://doi.org/10.1002/grl.50348

Waldrop, M. P., Chabot, C. L., Liebner, S., Holm, S., Snyder, M. W., Dillon, M., et al. (2023). Permafrost microbial communities and functional genes are structured by latitudinal and soil geochemical gradients. *The ISME Journal*, *17*(8), 1224–1235. https://doi.org/10.1038/s41396-023-01429-6

Walker, D. A., & Maier, H. A. (2008). Vegetation in the vicinity of Toolik Field Station, Alaska. In *Biological papers of the University of Alaska, No 28* (Vol. 1(63), p. 360).

Walker, D. A., Raynolds, M. K., Daniëls, F. J. A., Einarsson, E., Elvebakk, A., Gould, W. A., et al. (2005). The circumpolar Arctic vegetation map. *Journal of Vegetation Science*, *16*(3), 267–282. https://doi.org/10.1111/j.1654-1103.2005.tb02365.x

Ward, C. P., Bowen, J. C., Freeman, D. H., & Sharpless, C. M. (2021). Rapid and reproducible characterization of the wavelength dependence of aquatic photochemical reactions using light-emitting diodes. *Environmental Science and Technology Letters*, *8*(5), 437–442. https://doi.org/10.1021/acs.estlett.1c00172

Ward, C. P., & Cory, R. M. (2016). Complete and partial photo-oxidation of dissolved organic matter draining permafrost soils. *Environmental Science & Technology*, *50*(7), 3545–3553. https://doi.org/10.1021/acs.est.5b05354

Ward, C. P., & Cory, R. M. (2020). Assessing the prevalence, products, and pathways of dissolved organic matter partial photo-oxidation in arctic surface waters. *Environmental Sciences: Processes & Impacts*, *22*(5), 1214–1223. https://doi.org/10.1039/c9em00504h

Ward, C. P., Nalven, S. G., Crump, B. C., Kling, G. W., & Cory, R. M. (2017). Photochemical alteration of organic carbon draining permafrost soils shifts microbial metabolic pathways and stimulates respiration. *Nature Communications*, *8*(772), 1–7. https://doi.org/10.1038/s41467-017-00759-2

Wetzel, R. G., Hatcher, P. G., & Bianchi, T. S. (1995). Natural photolysis by ultraviolet irradiance of recalcitrant dissolved organic matter to simple substrates for rapidbacterial metabolism. *Limnology & Oceanography*, *40*(8), 1369–1380. https://doi.org/10.4319/lo.1995.40.8.1369

Whelan, T., Sackett, W. M., & Benedict, C. R. (1970). Carbon isotope discrimination in a plant possessing the C4 dicarboxylic acid pathway. *Biochemical and Biophysical Research Communications*, *41*(5), 1205–1210. https://doi.org/10.1016/0006-291X(70)90214-7

White, E. M., Vaughan, P. P., & Zepp, R. G. (2003). Role of the photo-Fenton reaction in the production of hydroxyl radicals and photobleaching of colored dissolved organic matter in a coastal river of the southeastern United States. *Aquatic Sciences*, *65*(4), 402–414. https://doi.org/10.1007/s00027-003-0675-4

Wild, B., Andersson, A., Broder, L., Vonk, J., Hugelius, G., McClelland, J. W., et al. (2019). Rivers across the Siberian Arctic unearth the patterns of carbon release from thawing permafrost. *Proceedings of the National Academy of Sciences of the United States of America*, *116*(21), 10280–10285. https://doi.org/10.1073/pnas.1811797116

Xie, H., Zafiriou, O. C., Cai, W. J., Zepp, R. G., & Wang, Y. (2004). Photooxidation and its effects on the carboxyl content of dissolved organic matter in two coastal rivers in the southeastern United States. *Environmental Science & Technology*, *38*(15), 4113–4119. https://doi.org/10.1021/es035407t

Xu, L., Roberts, M. L., Elder, K. L., Kurz, M. D., McNichol, A. P., Reddy, C. M., et al. (2021). Radiocarbon in dissolved organic carbon by UV oxidation: Procedures and blank characterization at NOSAMS. *Radiocarbon*, *63*(1), 357–374. https://doi.org/10.1017/RDC.2020.102

Zhang, S., Pavelsky, T. M., Arp, C. D., & Yang, X. (2021). Remote sensing of lake ice phenology in Alaska. *Environmental Research Letters*, *16*(6), 064007. https://doi.org/10.1088/1748-9326/abf965

Zhao, L., Zou, D., Hu, G., Du, E., Pang, Q., Xiao, Y., et al. (2020). Changing climate and the permafrost environment on the Qinghai–Tibet (Xizang) plateau. *Permafrost and Periglacial Processes*, *31*(3), 396–405. https://doi.org/10.1002/ppp.2056

References From the Supporting Information

Blair, N., Leu, A., Munoz, E., Olsen, J., Kwong, E., & Des Marais, D. (1985). Carbon isotopic fractionation in heterotrophic microbial metabolism. *Applied and Environmental Microbiology*, *50*(4), 996–1001. https://doi.org/10.1128/aem.50.4.996-1001.1985

Bockheim, J. G. (2007). Importance of cryoturbation in redistributing organic carbon in permafrost-affected soils. *Soil Science Society of America Journal*, *71*(4), 1335–1342. https://doi-org.proxy.lib.umich.edu/10.2136/sssaj2006.0414N

Boutton, T. (1996). Stable carbon isotope ratios of soil organic matter and their use as indicators of vegetation and climate change. In T. W. Boutton & S. Yamasaki (Eds.), *Mass Spectrometry of soils* (pp. 47–82). Marcel Dekker, Inc.

Bowen, J. C., Ward, C. P., Kling, G. W., & Cory, R. M. (2020). Arctic amplification of global warming strengthened by sunlight oxidation of permafrost carbon to CO_2. *Geophysical Research Letters*, *47*(12), 0–3. https://doi.org/10.1029/2020GL087085

Breecker, D. O., Bergel, S., Nadel, M., Tremblay, M. M., Osuna-Orozco, R., Larson, T. E., & Sharp, Z. D. (2015). Minor stable carbon isotope fractionation between respired carbon dioxide and bulk soil organic matter during laboratory incubation of topsoil. *Biogeochemistry*, *123*(1–2), 83–98. https://doi.org/10.1007/s10533-014-0054-3

DeNiro, M. J., & Epstein, S. (1978). Mechanism of carbon isotope fractionation associated with lipid synthesis. *Science*, *197*(4300), 261–263. https://doi.org/10.1126/science.327543

Eisner, W. R. (1991). Palynological analysis of a peat core from Imnavait Creek, the North Slope, Alaska. *Arctic*, *44*(4), 279–282. https://doi.org/10.14430/arctic1551

Hilman, B., Weiner, T., Haran, T., Masiello, C. A., Gao, X., & Angert, A. (2022). The apparent respiratory quotient of soils and tree stems and the processes that control it. *Journal of Geophysical Research: Biogeosciences*, *127*(3), e2021JG006676. https://doi.org/10.1029/2021JG006676

Hoehler, T., Losey, N. A., Gunsalus, R. P., & McInerney, M. J. (2010). Environmental constraints that limit methanogenesis. In K. N. Timmis (Ed.), *Handbook of hydrocarbon and lipid microbiology* (pp. 635–645). Springer.

Marion, G. M., & Oechel, W. (1993). Mid- to late-Holocene carbon balance in arctic Alaska and its implications for future global warming. *The Holocene*, *3*(3), 193–200. https://doi.org/10.1177/095968369300300301

Nakamura, K., Takai, Y., & Wada, E. (1990). Carbon isotopes of soil gases and related organic carbon in an agroecosystem with special reference to paddy field. In E. M. Durrance, E. M. Galimov, M. E. Hinkle, et al. (Eds.), *Geochemistry of gaseous elements and compounds* (pp. 455–484). Theoprastus Publications.

Nichols, J. E., Peteet, D. M., Frolking, S., & Karavias, J. (2017). A probabilistic method of assessing carbon accumulation rate at Imnavait Creek Peatland, Arctic Long Term Ecological Research Station, Alaska. *Journal of Quaternary Science*, *32*(5), 579–586. https://doi.org/10.1002/jqs.2952

Opsahl, S. P., & Zepp, R. G. (2001). Photochemically-induced alteration of stable carbon isotope ratios ($\delta^{13}C$) in terrigeneous dissolved organic carbon. *Geophysical Research Letters*, *28*(12), 2417–2420. https://doi.org/10.1029/2000GL012686

Quay, P. D., King, S. L., Lansdown, J. M., & Wilbur, D. O. (1988). Isotopic composition of methane released from wetlands: Implications for the increase in atmospheric methane. *Global Biogeochemical Cycles*, *2*(4), 385–397. https://doi.org/10.1029/GB002i004p00385

Ratti, M., Canonica, S., McNeill, K., Erickson, P. R., Bolotin, J., & Hofstetter, T. B. (2015). Isotope fractionation associated with the direct photolysis of 4-chloroaniline. *Environmental Science & Technology*, *49*(7), 4263–4273. https://doi.org/10.1021/es505784a

Rivkina, E., Shcherbakova, V., Laurinavichius, K., Petrovskaya, L., Krivushin, K., Kraev, G., et al. (2007). Biogeochemistry of methane and methanogenic archaea in permafrost. *FEMS Microbiology Ecology*, *61*(1), 1–15. https://doi.org/10.1111/j.1574-6941.2007.00315.x

Romanowicz, K. J., Crump, B. C., & Kling, G. W. (2021). Rainfall alters permafrost soil redox conditions, but meta-omics show divergent microbial community responses by tundra type in the arctic. *Soil Systems*, *5*(1), 17. https://doi.org/10.3390/soilsystems5010017

Santruckova, H., Bird, M. I., & Lloyd, J. (2000). Microbial processes and carbon-isotope fractionation in tropical and temperate grassland soils. *Functional Ecology*, *14*(1), 108–114. https://doi.org/10.1046/j.1365-2435.2000.00402.x

Shingubara, R., Sugimoto, A., Murase, J., Iwahana, G., Tei, S., Liang, M., et al. (2019). Multi-year effect of wetting on CH_4 flux at taiga-tundra boundary in northeastern Siberia deduced from stable isotope ratios of CH_4. *Biogeosciences*, *16*(3), 755–768. https://doi.org/10.5194/bg-16-755-2019

Vaughn, L. J. S., Conrad, M. E., Bill, M., & Torn, M. S. (2016). Isotopic insights into methane production, oxidation, and emissions in Arctic polygon tundra. *Global Change Biology*, *22*(10), 3487–3502. https://doi.org/10.1111/gcb.13281

Wedin, D. A., Tieszen, L. L., Dewey, B., & Pastor, J. (1995). Carbon isotope dynamics during grass decomposition and soil organic matter formation. *Ecology*, *76*(5), 1383–1392. https://doi.org/10.2307/1938142

Whiticar, M. J. (1999). Carbon and hydrogen isotope systematics of bacterial formation and oxidation of methane. *Chemical Geology*, *161*(1–2), 291–314. https://doi.org/10.1016/S0009-2541(99)00092-3

Willach, S., Lutze, H. V., Eckey, K., Löppenberg, K., Lüling, M., Wolvert, J., et al. (2018). Direct photolysis of sulfamethoxazole using various irradiation sources and wavelength ranges - Insights from degradation product analysis and compound-specific stable isotope analysis. *Environmental Science & Technology*, *52*(3), 1225–1233. https://doi.org/10.1021/acs.est.7b04744

Journal of Geophysical Research: Biogeosciences

Supporting Information for

Controls on the Respiration of Ancient Carbon Draining from Permafrost Soils into Sunlit Arctic Surface Waters

E. C. Rieb[1], C. A. Polik[1†], C. P. Ward[2], G. W. Kling[3], and R. M. Cory[1*]

[1]Department of Earth and Environmental Sciences, University of Michigan, Ann Arbor, Michigan, 48109. [2]Department of Marine Chemistry and Geochemistry, Woods Hole Oceanographic Institution, Woods Hole, MA, 02543. [3]Department of Ecology and Evolutionary Biology, University of Michigan, Ann Arbor, MI, 48109.

*Corresponding author: Rose Cory (rmcory@umich.edu)
†Currently at: Department of Ecology, Evolution, and Behavior, University of Minnesota, St. Paul, MN 55108

Contents of this file

Text S1. Supporting Methods

S1.1 Preparation of multiple leachates for tussock tundra and thermokarst soils

An original set of dark control samples for the thermokarst soil leachates was compromised due to substantial microbial respiration consuming dissolved organic carbon (DOC) in the dark control leachate as it sat at room temperature during light exposure experiments and prior to biological incubations (Step C in Fig. S2). To replace the compromised dark control thermokarst waters, a second leachate was prepared from the thermokarst soil on a different date using the same soil and leaching conditions. The original thermokarst soil leachate was used for the ultraviolet (UV) and visible light treatments and subsequent biological incubation, while the second thermokarst soil leachate was used for the dark treatment and subsequent biological incubation (see Table S2). See SI Section 2.3 for a discussion of differences in water chemistry between the two thermokarst leachates. For all other soils, no detectable microbial respiration occurred in the dark controls during light exposure experiments, and thus the same soil leachate was used for both the dark and light treatments. Microbial respiration in soil leachates from any site during light exposure was negligible because microbes remaining in the leachates after filtration likely do not survive the exposure to intense UV and visible light (Ward et al., 2017).

Separately, samples of the CO_2 from microbial respiration in the dark and visible light-exposed tussock tundra leachate were lost during preparation for isotopic analysis at the National Ocean Sciences Accelerator Mass Spectrometry (NOSAMS) Facility. Therefore, a second soil leachate was prepared from the tussock tundra soil using the same soil and leaching conditions, and all of the dark and light treatments and biological incubations for this soil leachate were repeated. Throughout the manuscript, the incomplete ^{14}C (UV and visible light treatments only) and ^{13}C (UV light treatment only) data from the original tussock tundra leachate (tussock tundra A) are presented along with the complete ^{13}C and ^{14}C data for all light and dark treatments from the second tussock tundra leachate (tussock tundra B).

S1.2 Statistical analyses

Statistical tests were used to determine whether light exposure of permafrost DOC resulted in significant changes in the amount or isotopic composition of CO_2 from microbial respiration, and whether the isotopic composition of CO_2 from microbial respiration changed significantly as a function of any other variables. Two-tailed, paired t-tests were conducted to determine significant differences in CO_2 from respiration, respiratory quotient, and $\Delta^{14}C$ and $\delta^{13}C$ of CO_2 from respiration in the light-exposed versus dark treatments. Statistical significance was defined as $p < 0.05$. T-tests were used to determine whether the slopes and intercepts of each least-squares regression in Figures 3, 4, and S4 were significantly different from zero.

S1.3 Quantifying the yield of products of DOC photodegradation

The wavelength-dependent yield of products of DOC photodegradation (including the additional or lesser amount of CO_2 from respiration of DOC after light exposure) per mole of light absorbed

by the light-absorbing fraction of DOC cannot be reported in this study. Calculating the yield of products of photodegradation requires quantifying the amount of light absorbed by DOC. The light exposure experiments in this study were not designed to allow reliable quantification of the amount of light absorbed by DOC for the following reasons. First, soil leachates were exposed to UV and visible LED lights in spherical quartz flasks, causing leachate in different regions of the flasks to be different distances away from the light source and to have different pathlengths through the water. Additionally, an array of multiple LEDs were used at each wavelength (UV and visible), resulting in non-uniform intensity of downwelling irradiance across the area of the chamber in which leachates were exposed to light. Therefore, the products of DOC photodegradation by UV and visible wavelengths of light are reported as concentrations in this study, rather than as yields.

S1.4 Quantifying methane concentrations in permafrost soil leachates

To help interpret the ^{13}C composition of CO_2 from microbial respiration of DOC in permafrost soil leachates, we report methane concentrations in permafrost soil leachates used in other work but prepared using similar methods as in this study. Details about the leachates and methane concentrations are summarized in Table S6 and discussed in SI Section 2.1.2.

Methane concentrations in one leachate of Imnavait wet sedge permafrost soil were quantified via the following methods. DOC was leached from wet sedge permafrost soil with the same soil to water ratio and leaching conditions as the wet sedge leachate used in this study, as detailed in Table S2. After leaching, this wet sedge soil leachate was passed through a MilliQ-rinsed 60 μm mesh screen to remove the largest particulates. Subsequently, the leachate was passed through MilliQ-rinsed 5 μm and 0.2- μm high-capacity Whatman cartridge filters (Step A in Fig. S2). After filtration, a subset of the 0.2-μm filtered leachate was treated as inoculum and stored at 4 °C until further use in biological incubations (Step B in Fig. S2). Another subset of the 0.2-μm filtered leachate was prepared as a dark-treated water (without corresponding light treatments) and allowed to warm from the 4 °C storage temperature to room temperature for ~24 hours prior to the start of dark treatments. Prior to the dark treatment, this soil leachate was placed in duplicate precombusted, 500-mL Pyrex bottles with gastight stoppers without headspace. These duplicate leachates were then stored in the dark at room temperature for 3 days (Step C in Fig. S2). After dark treatments, the duplicates of the dark-treated soil leachate were composited in a precombusted, glass bottle (Step D in Fig. S2) and stored overnight in the fridge at 4 °C. Finally, the composited, dark-treated leachate was mixed with 0.2-μm filtered leachate that had been treated as inoculum (Step D in Fig. S2) to achieve 20% inoculum by volume. Methane concentrations in the final leachate mixture (after Step D in Fig. S2) were measured on a membrane inlet mass spectrometer (MIMS).

Separately, methane concentrations in leachates of permafrost soils from four sites (Imnavait wet sedge, Toolik wet sedge, Imnavait tussock tundra, and Toolik tussock tundra; Table S6) were quantified via the following methods. Frozen permafrost soil from each site (3,660 g) was mixed with 15 L of MilliQ water in 5-gallon, MilliQ-rinsed HDPE buckets and allowed to leach in the

dark for ~36 hours at 4 °C. The leachates were then passed through MilliQ-rinsed 200 µm nitex mesh screens to remove the largest particulates. In triplicate, 500 mL of the leachate was added to jars containing 600 g of permafrost soil from the same site, and the jars were sealed with airtight lids containing a septum for gas sampling. The sealed jars were shaken thoroughly to allow dissolved gases from the permafrost leachate and soil mixture to equilibrate with gas in the headspace of the jar at 4 °C. Gas samples from the headspace of the incubation vessel were analyzed for methane via gas chromatography on a Shimadzu GC-14A gas chromatograph (Romanowicz et al., 2021). Dissolved methane concentrations in the permafrost leachates were calculated using Henry's Law and the partial pressure of methane in the headspace of the jar (Table S6).

S1.5 Mass balance calculations of the ^{13}C content of oxidized methane

A mass balance calculation was performed to estimate the ^{13}C composition of methane-derived CO_2 potentially produced during biological incubations in this study using the following equation:

$$\delta^{13}C_{CO_2} = f_{CO_2\text{-}CH_4}(\delta^{13}C_{CH_4}) + f_{CO_2\text{-}DOC}(\delta^{13}C_{DOC})$$

where $f_{CO_2\text{-}CH_4}$ and $f_{CO_2\text{-}DOC}$ are the fractions of the total CO_2 from respiration that are derived from methane and non-methane DOC, and $\delta^{13}C_{CH_4}$ and $\delta^{13}C_{DOC}$ are the ^{13}C isotopic compositions of methane and DOC in permafrost soils, respectively. $\delta^{13}C_{CO_2}$ is the net $\delta^{13}C$ of the total CO_2 produced during biological incubations, reported in Table 1. This calculation assumes that there are only two carbon sources for the CO_2 produced during each biological incubation experiment: methane and non-methane DOC. In order to give a conservative estimate of how ^{13}C-depleted the methane in permafrost leachates was, the fraction of the total CO_2 derived from methane was calculated using the maximum concentration of methane measured in permafrost soil leachates (1.2 µM; Table S6). This assumed that virtually all of the methane present was oxidized to CO_2. The fraction of the total CO_2 derived from non-methane DOC was calculated as the difference between the total CO_2 and the fraction derived from methane. A $\delta^{13}C$ value equal to that of the bulk DOC in each leachate (Table 1) was assigned to CO_2 derived from non-methane DOC. When solved for $\delta^{13}C_{CH_4}$, this calculation demonstrated that the methane in the permafrost leachates in this study would have to have $\delta^{13}C$ values of -120‰ or lower for oxidation of 1.2 µM methane to account for the highly depleted $\delta^{13}C$ of the total CO_2 produced during biological incubations of wet sedge and tussock tundra A leachates.

Because this calculation assumed complete oxidation of the initial methane present, any potential fractionation factor associated with aerobic oxidation of methane to CO_2 by methanotrophs in the incubations was disregarded. If less than all of the methane present were oxidized to CO_2, then fractionation during aerobic methane oxidation would produce further-^{13}C-depleted CO_2 relative to the methane substrate, with fractionation factors ranging widely from ~4 to 30‰ (Whiticar, 1999). Therefore, fractionation during oxidation of a smaller amount of the initial methane

present could potentially produce similarly ^{13}C-depleted CO_2 as complete oxidation of the initial methane present.

Text S2. Supporting Text

S2.1 Constraints on the age range of permafrost DOC respired to CO_2

Both the DOC leached from permafrost soils and the CO_2 from respiration of that DOC are mixtures of C compounds of different ages. Thus, while this study reports the average ^{14}C isotopic composition of the initial DOC and CO_2 from respiration, these $\Delta^{14}C$ values do not provide full information about the range of ^{14}C isotopic compositions present in either mixture. The exact distribution of ages within DOC draining from any permafrost soil is poorly characterized (Rogers et al., 2021). However, it is possible to place minimum and maximum constraints on the ages of DOC that could be present in leachates of permafrost soils in this study.

First, to constrain the oldest C that could be present in samples, most of the organic carbon accumulation in all landscape ages sampled in this study began after the end of the last glacial period and the start of the Holocene. For example, bulk organic carbon from peat near our Imnavait sampling sites is ~11,000 a BP at 160 cm depth and from ~ 5,000 to 8,000 a BP at the sampling depth of 85 cm at Imnavait Creek in this study (Eisner, 1991; macrofossil dates at these depths from a similar location are slightly younger but overall similar, Nichols et al., 2017). Therefore, even with the possibility of cryoturbation of older, deeper organic matter upward to the sampling depths in this study, the maximum age of this older organic carbon is ~12,000 a BP.

Second, to constrain the youngest C that could be present in samples, permafrost soils in this study were collected from 10-30 cm deeper than the maximum, active-layer thaw depths at Imnavait Creek and Toolik Lake (Romanowicz & Kling, 2022). Thus there should be little or no injection of modern C from above into our samples, even by cryoturbation. This is because cryoturbation operates at freeze-thaw fronts (Bockheim, 2007), and the main cryoturbation activity in North Slope tundra soils was during the mid-Holocene thermal maximum estimated from 9,500-6,500 a BP (Bockheim, 2007) or from 6,900-4,800 a BP (Marion & Oechel, 1993). Therefore, it is unlikely that much modern carbon from fresh plant material is present in our samples. The ages of organic carbon compounds in the permafrost DOC in this study, as well as the CO_2 from respiration of that DOC, should fall within a maximum range from several thousands of years old to ~12,000 a BP.

Despite these constraints, the DOC and CO_2 ages reported in this study are still averages of different organic compounds of different old ages. Therefore, while the average age of the CO_2 respired from light-exposed permafrost DOC is slightly younger than the average age of the CO_2 respired from permafrost DOC in the dark (Fig. 2a), it is not possible to determine exactly how light exposure affects the distribution of ages of permafrost DOC respired. However, for all soils and wavelengths for which light exposure increased respiration relative to dark controls, mass balance estimates were made of the age of the additional CO_2 from respiration of light-exposed

DOC. These estimates assumed that (1) for respiration of DOC up to the equivalent amount of CO_2 produced from the dark treatments, this CO_2 had the same average ^{14}C composition from respiration of both the dark and light-exposed DOC, and (2) any difference in the average ^{14}C composition of CO_2 respired between dark and light treatments (Fig. 2a) was due to a different ^{14}C composition of the additional CO_2 from the light treatment, compared to the dark control (Figs 1 and 2a, Tables 1 and S4). These mass balance calculations show that the average $\Delta^{14}C$ value of the additional CO_2 from respiration of the light-exposed DOC was -419‰ for UV-treated wet sedge, -265‰ for UV-treated tussock tundra B, and -400‰ and -376‰ for UV- and visible-treated thermokarst, respectively. These $\Delta^{14}C$ values are between 40‰ to 170‰ less ^{14}C-depleted (i.e., younger) than the bulk DOC at each site and correspond to ages of 2,400 to 4,300 a BP. Despite being younger than both the CO_2 from dark respiration and the bulk DOC, and similar to the youngest age of DOC expected at the depths in this study (described above), these ages for the additional CO_2 from respiration of light-exposed DOC are still thousands of years old. Thus, these calculations further support the conclusion in this study that permafrost DOC with ages greater than ~2,500 years old is labile to microbial respiration after exposure to sunlight.

S2.2 Multiple processes can contribute to microbial production of CO_2 that is ^{13}C-depleted relative to the bulk DOC

As discussed in the main text, the most ^{13}C-depleted CO_2 might reflect the isotopic signature of a small pool of the most labile fraction of permafrost DOC respired by microbes, composed of ^{13}C-depleted lipid and lignin-like DOC. However, respiration of ^{13}C-depleted DOC fractions cannot entirely account for the most depleted $\delta^{13}C$-CO_2 values reported here. For example, the CO_2 from respiration of the UV-exposed tussock tundra A permafrost DOC (-44.9‰) was more ^{13}C-depleted than expected for the most ^{13}C-depleted lipid or lignin-like components of the DOC pool (likely ranging from -38 to -31‰ for lipids and from -31 to -17‰ for lignin-like DOC; Benner et al., 1987; Bertoldi et al., 2014; Kling & Fry, 1992; McCallister & del Giorgio, 2008; Wedin et al., 1995). Furthermore, evidence suggests that microbes respire a range of compounds within permafrost DOC (Nalven et al., 2020; Ward et al., 2017), thus making it less likely that the most depleted CO_2 was from respiration of a single fraction of highly ^{13}C-depleted DOC. Here, we discuss the following processes that might contribute to the production of ^{13}C-depleted CO_2: (1) kinetic isotope fractionation during microbial respiration of DOC, (2) respiration of ^{13}C-depleted methane, and (3) respiration of ^{13}C-depleted DOC photoproducts.

The most likely explanation is that multiple of the processes discussed here contributed to the respiration of ^{13}C-depleted CO_2 in this work. The degree to which the ^{13}C isotopic composition of CO_2 produced by microbial respiration reflects different DOC sources (including different fractions of the DOC pool and methane) versus isotopic fractionation (including kinetic isotope effects associated with microbial respiration and photochemical isotope fractionation) remains poorly understood.

S2.2.1 Kinetic isotope fractionation during respiration of DOC

First, kinetic isotope effects occurring during microbial respiration can produce CO_2 that is ^{13}C-depleted relative to the organic carbon substrate for some organic compounds thought to be models for soil organic matter (Blair et al., 1985). However, a kinetic isotope effect is not well constrained for microbial respiration of DOC, in which there is a wide range of organic compounds with different ^{13}C compositions available for microbes to respire (Bowling et al., 2008). Additionally, the magnitude of the fractionation is likely variable and dependent on environmental factors including organic matter quality, microbial community composition, and microbial growth phase (Breecker et al., 2015; Crow et al., 2006; Santruckova et al., 2000). Thus, no study of DOC has confidently distinguished the effects of kinetic isotope fractionation and selective respiration of different soil fractions on the ^{13}C composition of CO_2 from respiration (Boutton, 1996; Breecker et al., 2015; Crow et al., 2006). However, the magnitude of the kinetic isotope effect is generally believed to be small during respiration of DOC (Boutton, 1996). Prior studies reporting kinetic isotope fractionation between CO_2 produced by microbial respiration and the bulk soil organic carbon estimate that CO_2 from respiration can range from <1 to 3‰ depleted in ^{13}C relative to the bulk soil organic carbon (e.g., Blair et al., 1985; Boutton, 1996; Breecker et al., 2015; DeNiro & Epstein, 1978; Nakamura et al., 1990; Santruckova et al., 2000). This fractionation factor is not large enough to explain why CO_2 produced by microbial respiration in this study was on average 8‰ depleted relative to the DOC (and with individual depletion values as low as 19‰). Therefore, kinetic isotope fractionation associated with microbial respiration is likely not the primary factor behind respiration of highly ^{13}C-depleted CO_2 from permafrost DOC in this study.

S2.2.2 Respiration of ^{13}C-depleted methane

Second, the ^{13}C-depleted composition of CO_2 from respiration of permafrost DOC might be a product of CO_2 derived from oxidation of ^{13}C-depleted methane. Biogenic methane in permafrost soils is highly ^{13}C-depleted, with $\delta^{13}C$ ranging from -99 to -40‰ (Quay et al., 1988; Rivkina et al., 2007; Shingubara et al., 2019; Vaughn et al., 2016). Additionally, studies of tundra soils from some of the same sites as in this study have shown that the native microbial communities in these soils contain methanotrophs capable of oxidizing methane to CO_2 under aerobic conditions similar to the incubations conducted in this study (Romanowicz et al., 2021). The effects of oxidation of methane on the isotopic composition of CO_2 from respiration are expected to have the greatest effect on $\delta^{13}C$-CO_2 values when the amount of CO_2 from respiration of DOC is low. Because the magnitude of respiration was low in this study, both in absolute magnitude (8-93 μM CO_2) and as a percent of the initial DOC (1-5%), the ^{13}C-depleted signature of CO_2 from methane oxidation could have been amplified here in comparison to incubations where a much larger percentage of the non-methane DOC was respired (Mann et al., 2015; Vonk et al., 2013). Consistent with this expectation, the most ^{13}C-depleted CO_2 was produced when respiration was the lowest (< 25 μM CO_2). In other studies, in which respiration is inferred to have produced up to ~5000 μM CO_2, the oxidation of the amount of methane typically measured in oxic permafrost

leachates would not have had a large influence on the overall ^{13}C composition of the CO_2 from respiration (Mann et al., 2015; Spencer et al., 2015). Additionally, oxidation of methane is consistent with the positive correlation between $\delta^{13}C$-CO_2 and the respiratory quotient (Fig. 3a). Oxidation of ^{13}C-depleted methane is expected to have the lowest respiratory quotient (~0.5) (Hilman et al., 2022) because carbon in methane is in its lowest oxidation state.

However, it is unlikely that oxidation of ^{13}C-depleted methane alone can account for the most depleted $\delta^{13}C$-CO_2 values reported here. Methane concentrations in permafrost leachates tested in this study are expected to be low, given the aerated conditions of the biological incubations conducted. Consistent with this expectation, permafrost leachates from the same sites and prepared similarly to those used in this study had dissolved methane concentrations of 1.2 μM or less after equilibrating with atmospheric gases over several days during filtering and storage before the start of the incubation (Table S6; K. Romanowicz, pers. comm.). These methane concentrations are not expected to increase during incubations, because production of methane by methanogens is unlikely under aerobic conditions (Hoehler et al., 2010). Assuming complete oxidation of the initial ~ 1 μM methane present in soil leachates to CO_2 during incubations, the initial methane would have to have $\delta^{13}C$ values of -120‰ or lower to produce the depleted $\delta^{13}C$-CO_2 values observed in this study (see SI Section 1.5). This value of -120‰ is well below even the most ^{13}C-depleted methane in permafrost soils in the literature (Quay et al., 1988; Rivkina et al., 2007; Shingubara et al., 2019; Vaughn et al., 2016) indicating that methane concentrations in soil leachates during incubations were likely too low for methane oxidation alone to produce the observed ^{13}C-depletion of the CO_2.

S2.2.3 Respiration of ^{13}C-depleted DOC photoproducts

A third possible explanation for the ^{13}C-depleted CO_2 from microbial respiration of some permafrost DOC is that photochemical isotope fractionation occurs during light exposure, producing new DOC photoproducts that are ^{13}C-depleted relative to the initial DOC. Prior work has shown that oxidation of DOC by sunlight produces CO_2 that is between 1 and 8‰ depleted in ^{13}C relative to the bulk DOC (Bowen et al., 2020; Opsahl & Zepp, 2001). However, this result has been interpreted as the selective oxidation of depleted lignin and tannin components of the DOC pool, rather than a kinetic isotope fractionation. A fractionation factor ranging from -4.8 to -1.2‰ has been reported for the photochemical breakdown of organic pollutants (Ratti et al., 2015; Willach et al., 2018). If light exposure similarly resulted in the production of ^{13}C-depleted photoproducts from DOC, then subsequent respiration of these photoproducts could contribute to microbial respiration and the production of highly ^{13}C-depleted CO_2 that was observed from the UV-treated wet sedge and tussock tundra A permafrost DOC.

In addition to the lack of evidence in the literature for photochemical isotopic fractionation of the DOC pool, there are several reasons why photochemical fractionation of the DOC pool is unlikely to explain the results of this study. First, respiration of ^{13}C-depleted CO_2 was not limited to the light-exposed permafrost DOC. Microbial respiration also produced CO_2 that was substantially ^{13}C-depleted relative to the DOC in the dark wet sedge treatment, where no

photochemical fractionation would have occurred. Additionally, the evidence suggests that photochemical fractionation would selectively release ^{13}C-depleted CO_2, leaving the remaining DOC ^{13}C-enriched (Bowen et al., 2020; Opsahl & Zepp, 2001). Therefore, light exposure might be expected to cause microbes to respire more ^{13}C-enriched DOC, which is opposite of the substantial ^{13}C-depletion of CO_2 from respiration of some of the light-exposed permafrost DOC. Finally, even for light-exposed DOC, the fractionation factors reported in past work for organic pollutants are not large enough to account for the full range of $\delta^{13}C$-CO_2 values, which were as much as 19‰ depleted relative to the DOC for the UV-treated tussock tundra A soil site. Therefore, while photochemical fractionation might contribute to the ^{13}C-depleted signature of CO_2 from respiration of some light-treated permafrost DOC, it alone cannot explain the full range of ^{13}C isotopic compositions of the CO_2 from respiration of DOC from all of the soil sites and treatments. Other factors (e.g., preferential respiration of ^{13}C-depleted DOC fractions, as previously described) must also be contributing to microbial production of ^{13}C-depleted CO_2.

S2.3 Different DOC concentrations in duplicate thermokarst leachates have minimal impact on light-dark differences in respiration

Of the duplicate leachates prepared from the thermokarst soil, the leachate used for the UV and visible light treatments had higher DOC than the leachate used for the dark treatment (1726 and 1328 μM DOC respectively; Table S2). Because the CO_2 production from respiration was significantly, positively correlated with initial DOC concentration in leachates in this study (Fig. S4), this difference in initial DOC concentration between the light-treated and dark thermokarst leachates likely had a small effect on the magnitude of CO_2 respired from light relative to dark treatments.

The approximately linear relationship between DOC concentrations in inoculated, dark-treated leachates from all of the sites at the start of incubations and the magnitude of CO_2 subsequently produced by respiration (data points for dark treatments in Fig. S4) was used to predict how much more CO_2 microbes would have respired from the dark-treated thermokarst leachate if it had a higher initial DOC concentration similar to that of the light treatments. If this were the case, microbial respiration in the hypothetical dark thermokarst leachate with higher DOC would produce 33 μM CO_2, a 12% increase in respiration compared to the 30 μM CO_2 measured from respiration in the actual dark thermokarst leachate with lower DOC (Table S4). If respiration from the dark thermokarst leachate had been higher by this amount, then respiration in the UV and visible light treatments of the thermokarst leachate would have been 184% and 125% higher than in the dark treatment, as compared to the values of 219% and 153% higher, respectively, that are reported in this study. Thus, the difference in DOC concentrations between light and dark treatments of the thermokarst leachate are not large enough to change the results for this soil site: both UV and visible light increased microbial respiration relative to thermokarst DOC respired in the dark, and the effect of both UV and visible light on the magnitude of microbial respiration was much greater for the thermokarst leachate than for any of the other two soil sites.

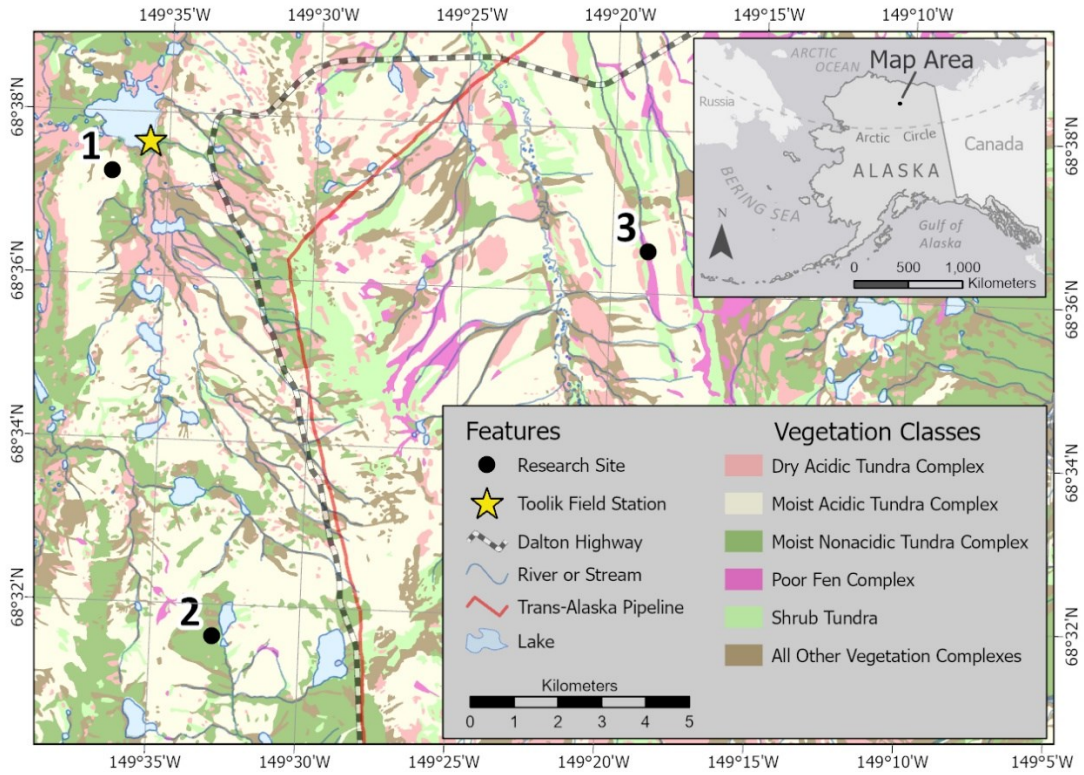

Figure S1. Map of sampling sites for permafrost soils collected from the dominant tundra types near Toolik Lake on the north slope of the Brooks Range in northern Alaska, USA. Permafrost soils were collected from Toolik Lake tussock tundra (1), from a thermokarst failure on the shore of Lake LTER 395 (2), and from Imnavait Creek wet sedge tundra (3). Major vegetation classes in this region, shown in color, were taken from Walker and Maier (2008). Wet sedge and tussock tundra vegetation are equivalent to the poor fen (dark pink) and moist acidic tundra (light tan) complexes shown on this map, respectively.

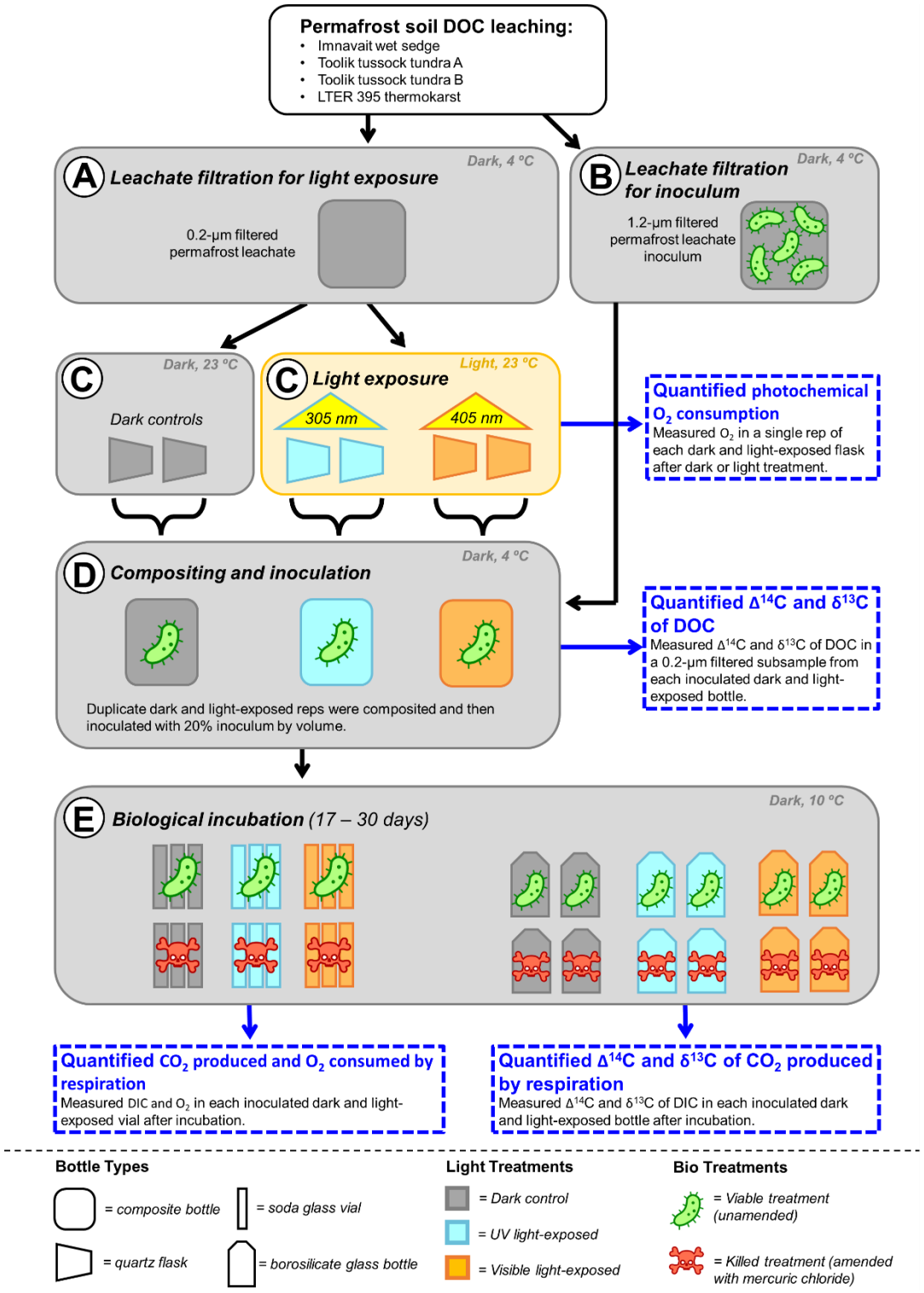

Figure S2. Experimental design for the light exposure and biological incubation experiments with permafrost soil DOC leachates. Four different permafrost leachates were prepared from permafrost soils collected from sites representing the dominant landscape ages and vegetation types of the low Arctic (Walker et al., 2005; Walker & Maier, 2008). Permafrost leachates from

each soil site were 0.2-µm filtered and stored in the dark at 4 °C until later use in light exposure experiments (Step A). A subset of each permafrost leachate was 1.2-µm filtered for inoculum and stored in the dark at 4 °C until further use in biological incubations (Step B). The 0.2-µm-filtered leachate from each soil site was either kept in the dark or exposed to either ultraviolet (UV; 305 nm) or visible (405 nm) LEDs at room temperature (Step C). Subsequently, the dark and light-exposed waters were inoculated with 1.2-µm filtered inoculum from Step B to achieve 20% inoculum by volume (Step D). Inoculated dark and light-exposed waters were incubated in the dark at 10 °C for between 17 to 30 days, alongside killed control treatments (Step E). At the end of biological incubations, the quantity and C isotopic composition of CO_2 from microbial respiration in all dark and light-exposed treatments was quantified.

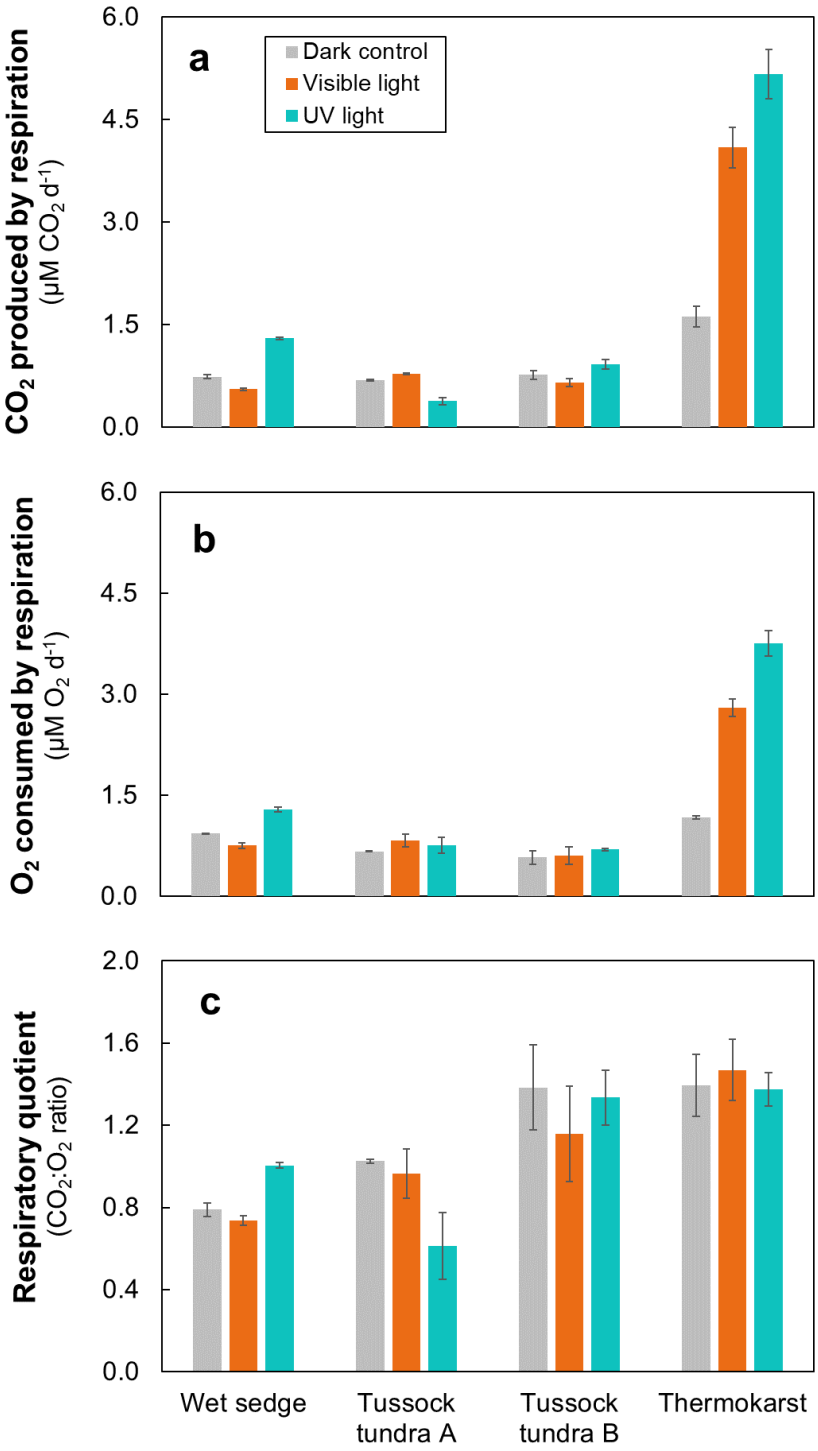

Figure S3. (a) Rates of CO_2 production by microbial respiration, (b) rates of O_2 consumption by microbial respiration, and (c) the respiratory quotient for microbial respiration of permafrost DOC collected from four soil sites and either kept in the dark (grey) or exposed to ultraviolet light (UV; blue) or visible light (405 nm, orange). All values are shown as the average ± 1 SE of experimental replicates (n = 3).

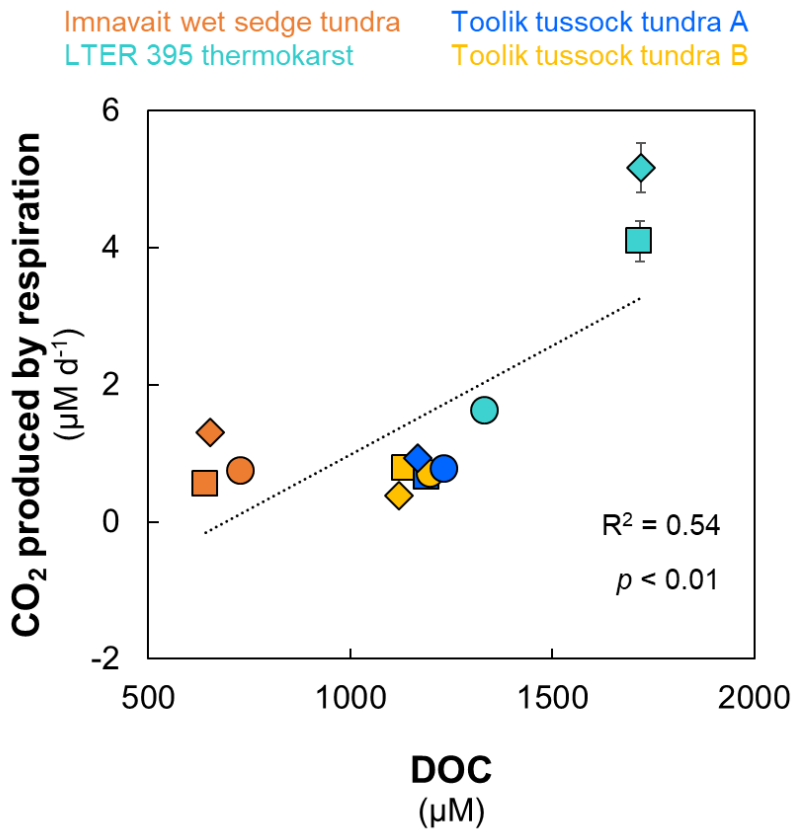

Figure S4. Rates of CO_2 production from microbial respiration of permafrost DOC kept in the dark (circle symbols), exposed to ultraviolet light (UV; 305 nm, diamond symbols), and exposed to visible light (405 nm, square symbols) versus the initial concentration of DOC in biological incubations of: Imnavait wet sedge tundra (orange symbols), Toolik tussock tundra A (dark blue symbols), Toolik tussock tundra B (yellow symbols), and LTER 395 thermokarst (teal symbols). Data were fit using a least-squares regression where $R^2 = 0.54$ and $p < 0.01$. All values on the y-axis are shown as the average ± 1 SE of experimental replicates ($n = 3$).

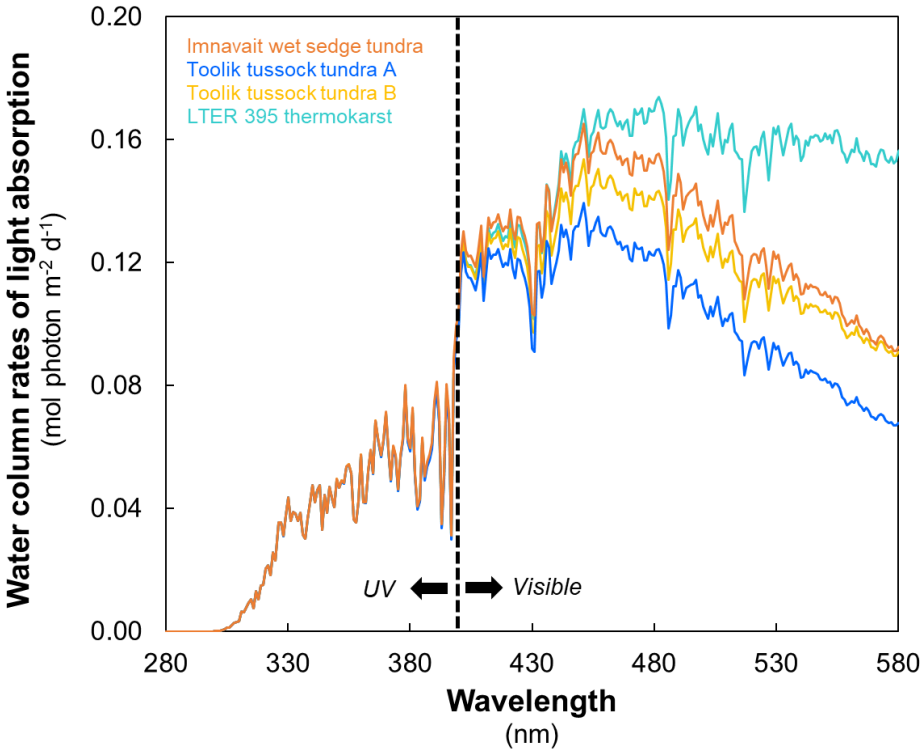

Figure S5. Wavelength-dependent water column rates of light absorption by the light-absorbing portion of permafrost DOC from: Imnavait wet sedge tundra (orange), Toolik tussock tundra A (dark blue), Toolik tussock tundra B (yellow), and LTER 395 thermokarst (teal). The black dashed line marks the transition between shorter ultraviolet (UV) wavelengths of light and longer visible wavelengths of light. Water column rates of light absorption were calculated using the wavelength-dependent light absorption by CDOM and the daily incoming photon flux spectrum measured on 21 June 2018 at Toolik Lake Field Station on the North Slope of Alaska (Cory et al., 2014). Rates of light absorption were integrated over the depth of Imnavait Creek, a small headwater creek draining tundra soils near the Toolik Lake Field Station.

Table S1

Date, location, and depth of permafrost soil collection

Permafrost soil	Landscape age (k a BP)	Glaciation	Date of soil collection	Latitude	Longitude	Depth of soil collection (cm)	Thaw depth (cm)
Imnavait wet sedge tundra	250	Sagavanirktok	19 Jul 2018	68°36’31.90"N	149°18’47.90"W	85	50
Toolik tussock tundra (A and B)	14	Itkillik I	17 Jul 2018	68°37’16.18"N	149°36’54.17"W	85	24
LTER 395 thermokarst	14	Itkillik I	17 Jun 2022	68°31'37.20"N	149°32'55.72"W	> 80	--

Note. Details from the Toolik tussock tundra and Imnavait wet sedge soils were previously reported (Bowen et al., 2020).

Table S2

Leaching conditions and chemical attributes of the permafrost leachates prepared from soils collected in 2018 and 2022

	Imnavait wet sedge tundra	Toolik tussock tundra A	Toolik tussock tundra B	LTER 395 thermokarst	LTER 395 thermokarst
	Before dark and UV + vis light treatments	*Before dark and UV + vis light treatments*	*Before dark and UV + vis light treatments*	*Before UV + vis light treatments*	*Before dark treatment*
Soil-to-water (g-soil L^{-1})	122	98	98	750	301
Thaw time (hr)	29	51	74	97	71
DOC leaching rate (μmol C g-soil^{-1} d^{-1})	4.1	5.3	4.1	0.6	1.5
pH	6.8	6.4	5.5	6.8	6.3
Specific conductivity (μS cm^{-1})	18	14	10	24	8
Total Fe (μM)	22.2	11.4	13.0	3.3	3.1
DOC (μM)	609	1095	1244	1726	1328
a_{305} (m^{-1})	31	19	19	23	19
$SUVA_{254}$ (L mg^{-1} C m^{-1})	3.42	1.23	1.05	1.02	1.07
Slope ratio (unitless)	0.69	0.89	0.86	1.03	1.19
Fluorescence index (unitless)	1.55	1.65	1.61	1.66	1.69

Table S3

Summary of the photon dose, photochemical O_2 consumption, and percentage of initial DOC oxidized by light during the light exposure of permafrost leachates

	Light treatment	Imnavait wet sedge tundra	Toolik tussock tundra A	Toolik tussock tundra B	LTER 395 thermokarst
Light exposure time (hr)	UV	35	34	20	45
	Visible	60	80	55	121
Experimental photon dose (mol photon m^{-2})	UV	4	4	2	5
	Visible	169	224	153	341
Photochemical O_2 consumption (μM)	UV	56	63	48	55
	Visible	55	58	48	37
DOC oxidized by light (%)	UV	9	6	4	3
	Visible	9	5	4	2

Note. DOC leached from permafrost soils was exposed to LEDs at 305 nm (UV) or 405 nm (visible) alongside DOC kept in the dark. The percentage of DOC oxidized by UV and visible light is calculated by dividing photochemical O_2 consumption by the concentration of DOC present in the initial leachate before light exposure.

Table S4

Summary of the incubation length, O_2 consumption by respiration, CO_2 production by respiration, and respiratory quotient during biological incubations

	Light treatment	Imnavait wet sedge tundra	Toolik tussock tundra A	Toolik tussock tundra B	LTER 395 thermokarst
Incubation length (days)	Dark	17	21	30	18
	UV	17	21	30	18
	Visible	17	21	30	18
Increase in total DIC during incubation (%)	Dark	12	19	30	25
	UV	19	8	33	49
	Visible	8	20	25	40
CO_2 production from respiration (μM)	Dark	12.5 ± 0.5	14.4 ± 0.3	22.9 ± 1.8	29.1 ± 2.7
	UV	22.0 ± 0.3	8.0 ± 1.1	27.6 ± 2.1	92.9 ± 6.5
	Visible	9.4 ± 0.3	16.3 ± 0.2	19.5 ± 1.7	73.6 ± 5.3
O_2 consumption from respiration (μM)	Dark	15.8 ± 0.1	14.0 ± 0.2	17.3 ± 3.0	21.0 ± 0.4
	UV	21.9 ± 0.6	15.9 ± 2.5	20.8 ± 0.5	67.7 ± 3.4
	Visible	12.8 ± 0.8	17.5 ± 2.0	18.1 ± 3.8	50.4 ± 2.3
Respiratory quotient (CO_2:O_2 molar ratio)	Dark	0.79 ± 0.03	1.03 ± 0.01	1.38 ± 0.21	1.39 ± 0.15
	UV	1.01 ± 0.01	0.61 ± 0.16	1.34 ± 0.13	1.37 ± 0.08
	Visible	0.74 ± 0.02	0.96 ± 0.12	1.16 ± 0.23	1.47 ± 0.15

Note. Values for O_2 consumption and CO_2 production from respiration are reported as the average ± 1 SE of experimental replicates (n = 3). The respiratory quotient is calculated as the ratio of CO_2 production to O_2 consumption during respiration and is reported as the average ± 1 SE of experimental replicates (n = 3).

Table S5

Accession numbers for the permafrost leachates analyzed for carbon isotopes of DOC or DIC at the National Ocean Sciences Accelerator Mass Spectrometry facility

Accession #	Permafrost soil	DOC or DIC analyzed for ^{14}C and ^{13}C	Light treatment	Biological incubation treatment	Rep #
OS-167259	Imnavait set sedge	DOC	Dark	N/A	--
OS-167261	Imnavait set sedge	DOC	UV	N/A	--
OS-167260	Imnavait set sedge	DOC	Visible	N/A	--
OS-167262	Toolik tussock tundra A	DOC	Dark	N/A	--
OS-167264	Toolik tussock tundra A	DOC	UV	N/A	--
OS-167263	Toolik tussock tundra A	DOC	Visible	N/A	--
OS-170337	Toolik tussock tundra B	DOC	Dark	N/A	--
OS-170339	Toolik tussock tundra B	DOC	UV	N/A	--
OS-170338	Toolik tussock tundra B	DOC	Visible	N/A	--
OS-170340	LTER 395 thermokarst	DOC	Dark	N/A	--
OS-170342	LTER 395 thermokarst	DOC	UV	N/A	--
OS-170341	LTER 395 thermokarst	DOC	Visible	N/A	--
OS-165577	Imnavait set sedge	DIC	Dark	Viable	1
OS-165578	Imnavait set sedge	DIC	Dark	Viable	2
OS-165579	Imnavait set sedge	DIC	Dark	Killed	1
OS-165580	Imnavait set sedge	DIC	Dark	Killed	2
OS-165581	Imnavait set sedge	DIC	UV	Viable	1
OS-165582	Imnavait set sedge	DIC	UV	Viable	2
OS-165583	Imnavait set sedge	DIC	UV	Killed	1
OS-165584	Imnavait set sedge	DIC	UV	Killed	2
OS-166079	Toolik tussock tundra A	DIC	UV	Viable	1
OS-166080	Toolik tussock tundra A	DIC	UV	Viable	2
OS-166081	Toolik tussock tundra A	DIC	UV	Killed	1
OS-166082	Toolik tussock tundra A	DIC	UV	Killed	2
OS-166075	Toolik tussock tundra A	DIC (^{14}C only)	Visible	Viable	1
OS-166076	Toolik tussock tundra A	DIC (^{14}C only)	Visible	Viable	2
OS-166077	Toolik tussock tundra A	DIC (^{14}C only)	Visible	Killed	1
OS-166078	Toolik tussock tundra A	DIC (^{14}C only)	Visible	Killed	2
OS-171035	Toolik tussock tundra B	DIC	Dark	Viable	1
OS-170851	Toolik tussock tundra B	DIC	Dark	Viable	2
OS-170850	Toolik tussock tundra B	DIC	Dark	Killed	1
OS-170849	Toolik tussock tundra B	DIC	Dark	Killed	2
OS-171040	Toolik tussock tundra B	DIC	UV	Viable	1
OS-171041	Toolik tussock tundra B	DIC	UV	Viable	2
OS-171042	Toolik tussock tundra B	DIC	UV	Killed	1
OS-171043	Toolik tussock tundra B	DIC	UV	Killed	2

OS-171036	Toolik tussock tundra B	DIC	Visible	Viable	1
OS-171037	Toolik tussock tundra B	DIC	Visible	Viable	2
OS-171038	Toolik tussock tundra B	DIC	Visible	Killed	1
OS-171039	Toolik tussock tundra B	DIC	Visible	Killed	2
OS-170852	LTER 395 thermokarst	DIC	Dark	Viable	1
OS-170853	LTER 395 thermokarst	DIC	Dark	Viable	2
OS-170854	LTER 395 thermokarst	DIC	Dark	Killed	1
OS-170855	LTER 395 thermokarst	DIC	Dark	Killed	2
OS-169974	LTER 395 thermokarst	DIC	UV	Viable	1
OS-170856	LTER 395 thermokarst	DIC	UV	Viable	2
OS-169976	LTER 395 thermokarst	DIC	UV	Killed	1
OS-169977	LTER 395 thermokarst	DIC	Visible	Viable	1
OS-169978	LTER 395 thermokarst	DIC	Visible	Viable	2
OS-169979	LTER 395 thermokarst	DIC	Visible	Killed	1
OS-169980	LTER 395 thermokarst	DIC	Visible	Killed	2

Note. Leachates of DOC from permafrost soils were prepared from soils collected in 2018 and 2022. Soil leachates were then either kept in the dark or exposed to LEDs at 305 nm (UV) and 405 nm (visible), and then inoculated with native microbial communities and incubated. At the start of the biological incubations, single replicates of the DOC after dark or light treatment and inoculation were analyzed for ^{14}C and ^{13}C. At the end of the biological incubations, the DIC in those waters was analyzed for ^{14}C and ^{13}C in duplicate.

Table S6

Methane concentrations in permafrost soil leachates

Permafrost soil	CH_4 (μM)	Measurement method
Imnavait wet sedge tundra	0.3	Leachate water analyzed for dissolved CH_4 via MIMS
Imnavait wet sedge tundra	1.2	Headspace gas sample analyzed for CH_4 via gas chromatography
Toolik wet sedge tundra	0.8	Headspace gas sample analyzed for CH_4 via gas chromatography
Imnavait tussock tundra	0.1	Headspace gas sample analyzed for CH_4 via gas chromatography
Toolik tussock tundra	0.4	Headspace gas sample analyzed for CH_4 via gas chromatography

Note. Soil cores were collected from some of the same arctic landscape ages and vegetation types as the leachates used in this study. Leachates were prepared using similar methods to the leachates in this study. K. Romanowicz, pers. comm.

References Cited

Benner, R., Fogel, M. L., Sprague, E. K., & Hodson, R. E. (1987). Depletion of ^{13}C in lignin and its implications for stable carbon isotope studies. *Nature, 329*, 708–710. https://doi.org/10.1038/329708a0

Bertoldi, D., Santato, A., Paolini, M., Barbero, A., Camin, F., Nicolini, G., & Larcher, R. (2014). Botanical traceability of commercial tannins using the mineral profile and stable isotopes. *Journal of Mass Spectrometry, 49*(9), 792–801. https://doi.org/10.1002/jms.3457

Blair, N., Leu, A., Munoz, E., Olsen, J., Kwong, E., & Des Marais, D. (1985). Carbon isotopic fractionation in heterotrophic microbial metabolism. *Applied and Environmental Microbiology, 50*(4), 996–1001. https://doi.org/10.1128/aem.50.4.996-1001.1985

Bockheim, J. G. (2007). Importance of cryoturbation in redistributing organic carbon in permafrost-affected soils. *Soil Science Society of America Journal, 71*(4), 1335-1342. https://doi-org.proxy.lib.umich.edu/10.2136/sssaj2006.0414N

Boutton, T. (1996). Stable carbon isotope ratios of soil organic matter and their use as indicators of vegetation and climate change. In T. W. Boutton and S. Yamasaki (Eds), *Mass Spectrometry of Soils.* (pp. 47–82). New York, Marcel Dekker, Inc.

Bowen, J. C., Ward, C. P., Kling, G. W., & Cory, R. M. (2020). Arctic amplification of global warming strengthened by sunlight oxidation of permafrost carbon to CO_2. *Geophysical Research Letters, 47*(12), 0–3. https://doi.org/10.1029/2020GL087085

Bowling, D. R., Pataki, D. E., & Randerson, J. T. (2008). Carbon isotopes in terrestrial ecosystem pools and CO_2 fluxes. *New Phytologist, 178*(1), 24–40. https://doi.org/10.1111/j.1469-8137.2007.02342.x

Breecker, D. O., Bergel, S., Nadel, M., Tremblay, M. M., Osuna-Orozco, R., Larson, T. E., et al. (2015). Minor stable carbon isotope fractionation between respired carbon dioxide and bulk soil organic matter during laboratory incubation of topsoil. *Biogeochemistry, 123*, 83-98. https://doi.org/10.1007/s10533-014-0054-3

Crow, S. E., Sulzman, E. W., Rugh, W. D., Bowden, R. D., & Lajtha, K. (2006). Isotopic analysis of respired CO_2 during decomposition of separated soil organic matter pools. *Soil Biology and Biochemistry, 38*(11), 3279–3291. https://doi.org/10.1016/j.soilbio.2006.04.007

DeNiro, M. J., & Epstein, S. (1978). Mechanism of carbon isotope fractionation associated with lipid synthesis. *Science, 197*(4300), 261-263. https://doi.org/10.1126/science.327543

Eisner, W. R. (1991). Palynological analysis of a peat core from Imnavait Creek, the North Slope, Alaska. *Arctic, 44*(4). 279-282. http://www.jstor.org/stable/40511285

Hilman, B., Weiner, T., Haran, T., Masiello, C. A., Gao, X., & Angert, A. (2022). The apparent respiratory quotient of soils and tree stems and the processes that control it. *Journal of Geophysical Research: Biogeosciences, 127*(3). https://doi.org/10.1029/2021JG006676

Hoehler, T., Losey, N. A., Gunsalus, R. P., & McInerney, M. J. (2010). Environmental constraints that limit methanogenesis. In K. N. Timmis (Ed) *Handbook of Hydrocarbon and Lipid Microbiology*. (pp. 635 – 645). Springer.

Kling, G. W., & Fry, B. (1992). Stable Isotopes and Planktonic Trophic Structure in Arctic Lakes. *Ecology, 73*(2), 561–566. https://doi.org/10.2307/1940762

Mann, P. J., Eglinton, T. I., McIntyre, C. P., Zimov, N., Davydova, A., Vonk, J. E., et al. (2015). Utilization of ancient permafrost carbon in headwaters of Arctic fluvial networks. *Nature Communications, 6*, 7856. https://doi.org/10.1038/ncomms8856

Marion, G. M., & Oechel, W. (1993). Mid- to late-Holocene carbon balance in arctic Alaska and its implications for future global warming. *Holocene, 3*(3), 193–200. https://doi.org/10.1177/095968369300300301

McCallister, S. L., & del Giorgio, P. A. (2008). Direct measurement of the $\delta^{13}C$ signature of carbon respired by bacteria in lakes: Linkages to potential carbon sources, ecosystem baseline metabolism, and CO_2 fluxes. *Limnology and Oceanography, 53*(4), 1204–1216. https://doi.org/10.4319/lo.2008.53.4.1204

Nakamura, K., Takai, Y., & Wada, E. (1990). Carbon isotopes of soil gases and related organic carbon in an agroecosystem with special reference to paddy field. In E. M. Durrance, E. M. Galimov, M. E. Hinkle, et al. (Eds) *Geochemistry of Gaseous Elements and Compounds*. (pp. 455 – 484). Athens, Theoprastus Publications.

Nalven, S. G., Ward, C. P., Payet, J. P., Cory, R. M., Kling, G. W., Sharpton, T. J., et al. (2020). Experimental metatranscriptomics reveals the costs and benefits of dissolved organic matter photo-alteration for freshwater microbes. *Environmental Microbiology, 22*(8), 3505-3521. https://doi.org/10.1111/1462-2920.15121

Nichols, J. E., Peteet, D. M., Frolking, S. & Karavias, J. (2017). A probabilistic method of assessing carbon accumulation rate at Imnavait Creek Peatland, Arctic Long Term Ecological Research Station, Alaska. *J. Quaternary Science*, *32*(5), 579-586. https://doi.org/10.1002/jqs.2952

Opsahl, S. P., & Zepp, R. G. (2001). Photochemically-induced alteration of stable carbon isotope ratios ($\delta^{13}C$) in terrigeneous dissolved organic carbon. *Geophysical Research Letters, 28*(12), 2417–2420. https://doi.org/10.1029/2000GL012686

Quay, P. D., King, S. L., Lansdown, J. M., & Wilbur, D. O. (1988). Isotopic composition of methane released from wetlands: Implications for the increase in atmospheric methane. *Global Biogeochemical Cycles, 2*(4), 385–397. https://doi.org/10.1029/GB002i004p00385

Ratti, M., Canonica, S., McNeill, K., Erickson, P. R., Bolotin, J., Hofstetter, & T. B. (2015). Isotope fractionation associated with the direct photolysis of 4-chloroaniline. *Environmental Science & Technology, 49*(7), 4263–4273. https://doi.org/10.1021/es505784a

Rivkina, E., Shcherbakova, V., Laurinavichius, K., Petrovskaya, L., Krivushin, K., Kraev, G., et

al. (2007). Biogeochemistry of methane and methanogenic archaea in permafrost. *FEMS Microbiology Ecology, 61*(1), 1–15. https://doi.org/10.1111/j.1574-6941.2007.00315.x

Rogers, J. A., Galy, V., Kellerman, A. M., Chanton, J. P., Zimov, N., & Spencer, R. G. M. (2021). Limited presence of permafrost dissolved organic matter in the Kolyma River, Siberia revealed by ramped oxidation. *Journal of Geophysical Research: Biogeosciences, 126*(7). https://doi.org/10.1029/2020JG005977

Romanowicz, K. J., Crump, B. C., & Kling, G. W. (2021). Rainfall alters permafrost soil redox conditions, but meta-omics show divergent microbial community responses by tundra type in the arctic. *Soil Systems, 5*(1), 17. https://doi.org/10.3390/soilsystems5010017

Romanowicz, J. K., & Kling, G. W. (2022). Summer thaw duration is a strong predictor of the soil microbiome and its response to permafrost thaw in arctic tundra. *Environmental Microbiology, 24*(12), 6220-6237. DOI: 10.1111/1462-2920.16218

Santruckova, H., Bird, M. I., & Lloyd, J. (2000). Microbial processes and carbon-isotope fractionation in tropical and temperate grassland soils. *Functional Ecology, 14*(1), 108–114. https://doi.org/10.1046/j.1365-2435.2000.00402.x

Shingubara, R., Sugimoto, A., Murase, J., Iwahana, G., Tei, S., Liang, M., et al. (2019). Multi-year effect of wetting on CH_4 flux at taiga-tundra boundary in northeastern Siberia deduced from stable isotope ratios of CH_4. *Biogeosciences, 16*(3), 755-768. https://doi.org/10.5194/bg-16-755-2019

Spencer, R. G. M., Mann, P. J., Dittmar, T., Eglinton, T. I., McIntyre, C., Holmes, R. M., et al. (2015). Detecting the signature of permafrost thaw in Arctic rivers. *Geophysical Research Letters, 42*(8), 2830–2835. https://doi.org/10.1002/2015GL063498

Vaughn, L. J. S., Conrad, M. E., Bill, M., & Torn, M. S. (2016). Isotopic insights into methane production, oxidation, and emissions in Arctic polygon tundra. *Global Change Biology, 22*(10), 3487–3502. https://doi.org/10.1111/gcb.13281

Vonk, J. E., Mann, P. J., Davydov, S., Davydova, A., Spencer, R. G. M., Schade, J., et al. (2013). High biolability of ancient permafrost carbon upon thaw. *Geophysical Research Letters, 40*(11), 2689–2693. https://doi.org/10.1002/grl.50348

Walker, D. A., & Maier, H. A. (2008). Vegetation in the vicinity of Toolik Field Station, Alaska. Fairbanks, AK. *Biological Papers of the University of Alaska, No 28, 1*(63), 360.

Walker, D. A., Raynolds, M. K., Daniëls, F. J. A., Einarsson, E., Elvebakk, A, Gould, W. A., et al. (2005). The circumpolar Arctic vegetation map. *Journal of Vegetation Science, 16*(3), 267–282. https://doi.org/10.1111/j.1654-1103.2005.tb02365.x

Ward, C. P., Nalven, S. G., Crump, B. C., Kling, G. W., & Cory, R. M. (2017). Photochemical alteration of organic carbon draining permafrost soils shifts microbial metabolic pathways and stimulates respiration. *Nature Communications, 8*(772), 1–7. https://doi.org/10.1038/s41467-017-00759-2

Wedin, D. A., Tieszen, L. L., Dewey, B., & Pastor, J. (1995). Carbon isotope dynamics during grass decomposition and soil organic matter formation. *Ecology, 76*(5), 1383-1392. https://doi.org/10.2307/1938142

Whiticar, M. J. (1999). Carbon and hydrogen isotope systematics of bacterial formation and oxidation of methane. *Chemical Geology, 161*(1-2), 291–314. https://doi.org/10.1016/S0009-2541(99)00092-3

Willach, S., Lutze, H. V., Eckey, K., Löppenberg, K., Lüling, M., Wolvert, J., et al. (2018). Direct photolysis of sulfamethoxazole using various irradiation sources and wavelength ranges - Insights from degradation product analysis and compound-specific stable isotope analysis. *Environmental Science & Technology, 52*(3), 1225–1233. https://doi.org/10.1021/acs.est.7b04744